CHAPTER

3

Physical Properties of Seawater

3.1. MOLECULAR PROPERTIES OF WATER

Many of the unique characteristics of the ocean can be ascribed to the nature of water itself. Consisting of two positively charged hydrogen ions and a single negatively charged oxygen ion, water is arranged as a polar molecule having positive and negative sides. This molecular polarity leads to water's high dielectric constant (ability to withstand or balance an electric field). Water is able to dissolve many substances because the polar water molecules align to shield each ion, resisting the recombination of the ions. The ocean's salty character is due to the abundance of dissolved ions.

The polar nature of the water molecule causes it to form polymer-like chains of up to eight molecules. Approximately 90% of the water molecules are found in these chains. Energy is required to produce these chains, which is related to water's heat capacity. Water has the highest heat capacity of all liquids except ammonia. This high heat capacity is the primary reason the ocean is so important in the world climate system. Unlike the land and atmosphere, the ocean stores large amounts of heat energy it receives from the sun. This heat is carried by ocean currents, exporting or importing heat to various regions. Approximately 90% of the anthropogenic heating associated with global climate change is stored in the oceans, because water is such an effective heat reservoir (see Section S15.6 located on the textbook Web site http://booksite.academicpress.com/DPO/; "S" denotes supplemental material).

As seawater is heated, molecular activity increases and thermal expansion occurs, reducing the density. In freshwater, as temperature increases from the freezing point up to about 4°C, the added heat energy forms molecular chains whose alignment causes the water to shrink, increasing the density. As temperature increases above this point, the chains break down and thermal expansion takes over; this explains why fresh water has a density maximum at about 4°C rather than at its freezing point. In seawater, these molecular effects are combined with the influence of salt, which inhibits the formation of the chains. For the normal range of salinity in the ocean, the maximum density occurs at the freezing point, which is depressed to well below 0°C (Figure 3.1).

Water has a very high heat of evaporation (or heat of vaporization) and a very high heat of fusion. The heat of vaporization is the amount of energy required to change water from a liquid to a gas; the heat of fusion is the amount of energy required to change water from a solid to a liquid. These quantities are relevant for our climate as water changes state from a liquid in the ocean to water vapor in the atmosphere and to ice at polar latitudes. The heat energy

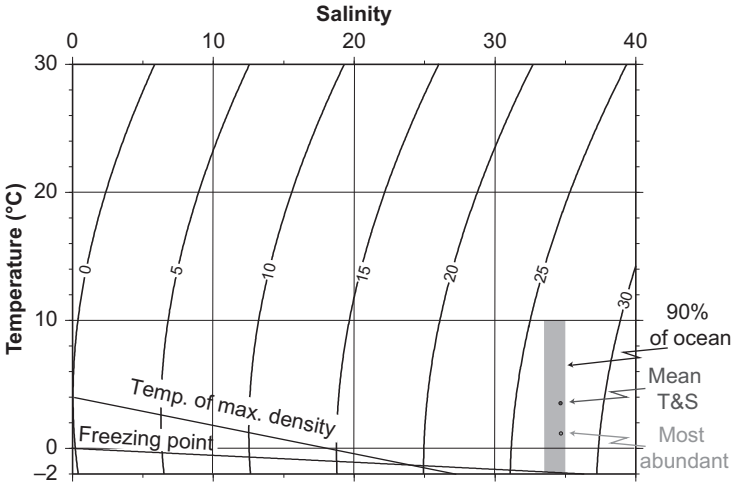

FIGURE 3.1 Values of density σ_t (curved lines) and the loci of maximum density and freezing point (at atmospheric pressure) for seawater as functions of temperature and salinity. The full density ρ is $1000 + \sigma_t$ with units of kg/m^3.

involved in these state changes is a factor in weather and in the global climate system.

Water's chain-like molecular structure also produces its high surface tension. The chains resist shear, giving water a high viscosity for its atomic weight. This high viscosity permits formation of surface *capillary waves*, with wavelengths on the order of centimeters; the restoring forces for these waves include surface tension as well as gravity. Despite their small size, capillary waves are important in determining the frictional stress between wind and water. This stress generates larger waves and propels the frictionally driven circulation of the ocean's surface layer.

3.2. PRESSURE

Pressure is the normal force per unit area exerted by water (or air in the atmosphere) on both sides of the unit area. The units of force are (mass $\times$ length/time^2). The units of pressure are (force/length^2) or (mass/[length $\times$ time^2]). Pressure units in centimeters-gram-second (cgs) are dynes/cm^2 and in meter-kilogram-second (mks) they are Newtons/m^2. A special unit for pressure is the Pascal, where 1 Pa = 1 N/m^2. Atmospheric pressure is usually measured in bars where 1 bar = 10^6 dynes/cm^2 = 10^5 Pa. Ocean pressure is usually reported in decibars where 1 dbar = 0.1 bar = 10^5 dyne/cm^2 = 10^4 Pa.

The force due to pressure arises when there is a difference in pressure between two points. The force is directed from high to low pressure. Hence we say the force is oriented "down the pressure gradient" since the gradient is directed from low to high pressure. In the ocean, the downward force of gravity is mostly balanced by an upward pressure gradient force; that is, the water is not accelerating downward. Instead, it is kept from collapsing by the upward pressure gradient force. Therefore pressure increases with increasing depth. This balance of downward gravity force and upward pressure gradient force, with no motion, is called *hydrostatic balance* (Section 7.6.1).

The pressure at a given depth depends on the mass of water lying above that depth. A pressure change of 1 dbar occurs over a depth change of slightly less than 1 m (Figure 3.2 and Table 3.1). Pressure in the ocean thus varies from near zero (surface) to 10,000 dbar (deepest). Pressure

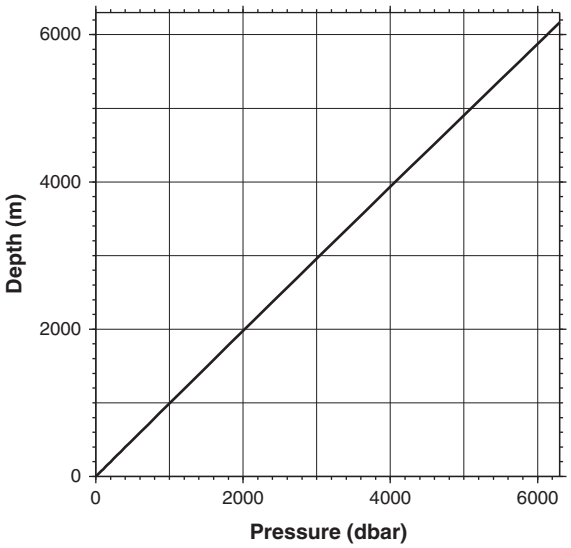

FIGURE 3.2 The relation between depth and pressure, using a station in the northwest Pacific at 41° 53′N, 146° 18′W.

TABLE 3.1 Comparison of Pressure (dbar) and Depth (m) at Standard Oceanographic Depths Using the UNESCO (1983) Algorithms

Pressure (dbar)	Depth (m)	Difference (%)
0	0	0
100	99	1
200	198	1
300	297	1
500	495	1
1000	990	1
1500	1453	1.1
2000	1975	1.3
3000	2956	1.5
4000	3932	1.7
5000	4904	1.9
6000	5872	2.1

Percent difference = (pressure − depth)/pressure × 100%.

is usually measured in conjunction with other seawater properties such as temperature, salinity, and current speeds. The properties are often presented as a function of pressure rather than depth.

Horizontal pressure gradients drive the horizontal flows in the ocean. For large-scale currents (of horizontal scale greater than a kilometer), the horizontal flows are much stronger than their associated vertical flows and are usually geostrophic (Chapter 7). The horizontal pressure differences that drive the ocean currents are on the order of one decibar over hundreds or thousands of kilometers. This is much smaller than the vertical pressure gradient, but the latter is balanced by the downward force of gravity and does not drive a flow. Horizontal variations in mass distribution create the horizontal variation in pressure in the ocean. The pressure is greater where the water column above a given depth is heavier either because it is higher density or because it is thicker or both.

Pressure is usually measured with an electronic instrument called a transducer. The accuracy and precision of pressure measurements is high enough that other properties such as temperature, salinity, current speeds, and so forth can be displayed as a function of pressure. However, the accuracy, about 3 dbar at depth, is not sufficient to measure the horizontal pressure gradients. Therefore other methods, such as the geostrophic method, or direct velocity measurements, must be used to determine the actual flow. Prior to the 1960s and 1970s, pressure was measured using a pair of mercury thermometers, one of which was in a vacuum ("protected" by a glass case) and not affected by pressure while the other was exposed to the water ("unprotected") and affected by pressure, as described in the following section. More information about these instruments and methods is provided in Section S6.3 of the supplementary materials on the textbook Web site.

3.3. THERMAL PROPERTIES OF SEAWATER: TEMPERATURE, HEAT, AND POTENTIAL TEMPERATURE

One of the most important physical characteristics of seawater is its temperature. Temperature was one of the first ocean parameters to be measured and remains the most widely observed. In most of the ocean, temperature is the primary determinant of density; salinity is of primary importance mainly in high latitude regions of excess rainfall or sea ice processes (Section 5.4). In the mid-latitude upper ocean (between the surface and 500 m), temperature is the primary parameter determining sound speed. (Temperature measurement techniques are described in Section S6.4.2 of the supplementary materials on the textbook Web site.)

The relation between temperature and heat content is described in Section 3.3.2. As a parcel of water is compressed or expanded, its temperature changes. The concept of "potential temperature" (Section 3.3.3) takes these pressure effects into account.

3.3.1. Temperature

Temperature is a thermodynamic property of a fluid, due to the activity or energy of molecules and atoms in the fluid. Temperature is higher for higher energy or heat content. Heat and temperature are related through the specific heat (Section 3.3.2).

Temperature (T) in oceanography is usually expressed using the Celsius scale (°C), except in calculations of heat content, when temperature is expressed in degrees Kelvin (K). When the heat content is zero (no molecular activity), the temperature is absolute zero on the Kelvin scale. (The usual convention for meteorology is degrees Kelvin, except in weather reporting, since atmospheric temperature decreases to very low values in the stratosphere and above.) A change of 1°C is the same as a change of 1 K. A temperature of 0°C is equal to 273.16 K. The range of temperature in the ocean is from the freezing point, which is around −1.7°C (depending on salinity), to a maximum of around 30°C in the tropical oceans. This range is considerably smaller than the range of air temperatures. As for all other physical properties, the temperature scale has been refined by international agreement. The temperature scale used most often is the International Practical Temperature Scale of 1968 (IPTS-68). It has been superseded by the 1990 International Temperature Scale (ITS-90). Temperatures should be reported in ITS-90, but all of the computer algorithms related to the equation of state that date from 1980 predate ITS-90. Therefore, ITS-90 temperatures should be converted to IPTS-68 by multiplying ITS-90 by 0.99976 before using the 1980 equation of state subroutines.

The ease with which temperature can be measured has led to a wide variety of oceanic and satellite instrumentation to measure ocean temperatures (see supplementary material in Section S6.4.2 on the textbook Web site). Mercury thermometers were in common use from the late 1700s through the 1980s. Reversing (mercury) thermometers, invented by Negretti and Zamba in 1874, were used on water sample bottles through the mid-1980s. These thermometers have ingenious glasswork that cuts off the mercury column when the thermometers are flipped upside down by the shipboard observer, thus recording the temperature at depth. The accuracy and precision of reversing thermometers is 0.004 and 0.002°C. Thermistors are now used for most in situ measurements. The best thermistors used most often in oceanographic instruments have an accuracy of 0.002°C and precision of 0.0005−0.001°C.

Satellites detect thermal infrared electromagnetic radiation from the sea surface; this radiation is related to temperature. Satellite sea surface temperature (SST) accuracy is about 0.5−0.8 K, plus an additional error due to the

presence or absence of a very thin (10 μm) skin layer that can reduce the desired bulk (1–2 m) observation of SST by about 0.3 K.

3.3.2. Heat

The heat content of seawater is its thermodynamic energy. It is calculated using the measured temperature, measured density, and the specific heat of seawater. The specific heat is a thermodynamic property of seawater expressing how heat content changes with temperature. Specific heat depends on temperature, pressure, and salinity. It is obtained from formulas that were derived from laboratory measurements of seawater. Tables of values or computer subroutines supplied by UNESCO (1983) are available for calculating specific heat. The heat content per unit volume, Q, is computed from the measured temperature using

$$Q = \rho c_p T \tag{3.1}$$

where T is temperature in degrees Kelvin, ρ is the seawater density, and c_p is the specific heat of seawater. The mks units of heat are Joules, that is, units of energy. The rate of time change of heat is expressed in Watts, where 1 W = 1 J/sec. The classical determinations of the specific heat of seawater were reported by Thoulet and Chevallier (1889). In 1959, Cox and Smith (1959) reported new measurements estimated to be accurate to 0.05%, with values 1 to 2% higher than the old ones. A further study (Millero, Perron, & Desnoyers, 1973) yielded values in close agreement with those of Cox and Smith.

The flux of heat through a surface is defined as the amount of energy that goes through the surface per unit time, so the mks units of heat flux are W/m^2. The heat flux between the atmosphere and ocean depends in part on the temperature of the ocean and atmosphere. Maps of heat flux are based on measurements of the conditions that cause heat exchange (Section 5.4). As a simple example, what heat loss from a 100 m thick layer of the ocean is needed to change the temperature by 1°C in 30 days? The required heat flux is $\rho c_p \Delta T\ V/\Delta t$. Typical values of seawater density and specific heat are about 1025 kg/m^3 and 3850 J/(kg °C). V is the volume of the 100 m thick layer, which is 1 m^2 across, and Δt is the amount of time (sec). The calculated heat change is 152 W. The heat flux through the surface area of 1 m^2 is thus about 152 W/m^2. In Chapter 5 all of the components of ocean heat flux and their geographic distributions are described.

3.3.3. Potential Temperature

Seawater is almost, but not quite, incompressible. A pressure increase causes a water parcel to compress slightly. This increases the temperature in the water parcel if it occurs without exchange of heat with the surrounding water (*adiabatic* compression). Conversely if a water parcel is moved from a higher to a lower pressure, it expands and its temperature decreases. These changes in temperature are unrelated to surface or deep sources of heat. It is often desirable to compare the temperatures of two parcels of water that are found at different pressures. *Potential temperature* is defined as the temperature that a water parcel would have if moved adiabatically to another pressure. This effect has to be considered when water parcels change depth.

The *adiabatic lapse rate* or *adiabatic temperature gradient* is the change in temperature per unit change in pressure for an adiabatic displacement of a water parcel. The expression for the lapse rate is

$$\Gamma(S, T, p) = \left.\frac{\partial T}{\partial p}\right|_{heat} \tag{3.2}$$

where S, T, and p are the measured salinity, temperature, and pressure and the derivative

is taken holding heat content constant. Note that both the compressibility and the adiabatic lapse rate of seawater are functions of temperature, salinity, and pressure. The adiabatic lapse rate was determined for seawater through laboratory measurements. Since the full equation of state of seawater is a complicated function of these quantities, the adiabatic lapse rate is also a complicated polynomial function of temperature, salinity, and pressure. In contrast, the lapse rate for ideal gases can be derived from basic physical principles; in a dry atmosphere the lapse rate is approximately 9.8°C/km. The lapse rate in the ocean, about 0.1 to 0.2°C/km, is much smaller since seawater is much less compressible than air. The lapse rate is calculated using computer subroutines based on UNESCO (1983).

The potential temperature is (Fofonoff, 1985):

$$\theta(S,T,p) = T + \int_{p}^{pr} \Gamma(S,T,p)dp \qquad (3.3)$$

where S, T, and p are the measured (in situ) salinity, temperature, and pressure, Γ is the adiabatic lapse rate, and θ is the temperature that a water parcel of properties (S, T, p) would have if moved adiabatically and without change of salinity from an initial pressure p to a reference pressure p_r where p_r may be greater or less than p. The integration above can be carried out in a single step (Fofonoff, 1977). An algorithm for calculating θ is given by UNESCO (1983), using the UNESCO adiabatic lapse rate (Eq. 3.2); computer subroutines in a variety of different programming languages are readily available. The usual convention for oceanographic studies is to reference potential temperature to the sea surface. When defined relative to the sea surface, potential temperature is always lower than the actual measured temperature, and only equal to temperature at the sea surface. (On the other hand, when calculating potential density referenced to a pressure other than sea surface pressure, potential temperature must also be referenced to the same pressure; see Section 3.5.)

As an example, if a water parcel of temperature 5°C and salinity 35.00 were lowered adiabatically from the surface to a depth of 4000 m, its temperature would increase to 5.45°C due to compression. The potential temperature relative to the sea surface of this parcel is always 5°C, while its measured, or in situ, temperature at 4000 m is 5.45°C. Conversely, if its temperature was 5°C at 4000 m depth and it was raised adiabatically to the surface, its temperature would change to 4.56°C due to expansion. The potential temperature of this parcel relative to the sea surface is thus 4.56°C. Temperature and potential temperature referenced to the sea surface from a profile in the northeastern North Pacific are shown in Figure 3.3. Compressibility itself depends on temperature (and salinity), as discussed in Section 3.5.4.

3.4. SALINITY AND CONDUCTIVITY

Seawater is a complicated solution containing the majority of the known elements. Some of the more abundant components, as percent of total mass of dissolved material, are chlorine ion (55.0%), sulfate ion (7.7%), sodium ion (30.7%), magnesium ion (3.6%), calcium ion (1.2%), and potassium ion (1.1%) (Millero, Feistel, Wright, & McDougall, 2008). While the total concentration of dissolved matter varies from place to place, the ratios of the more abundant components remain almost constant. This "law" of constant proportions was first proposed by Dittmar (1884), based on 77 samples of seawater collected from around the world during the Challenger Expedition (see Chapter S1, Section S1.2, on the textbook Web site), confirming a hypothesis from Forchhammer (1865).

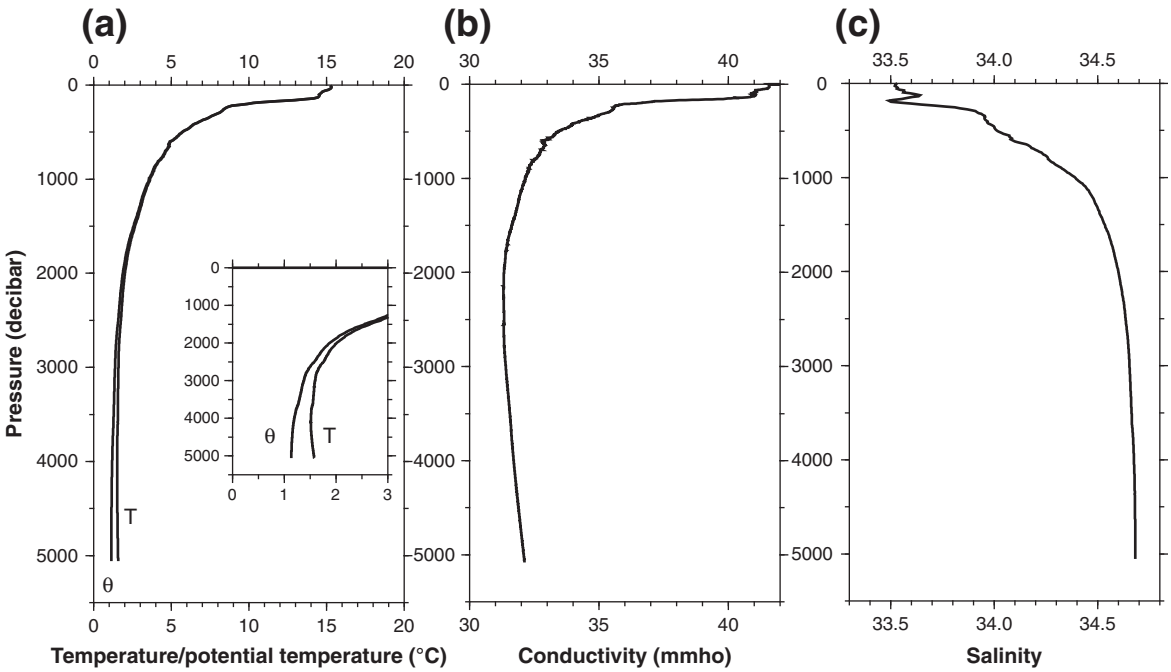

FIGURE 3.3 (a) Potential temperature (θ) and temperature (T) (°C), (b) conductivity (mmho), and (c) salinity in the northeastern North Pacific (36° 30′N, 135°W).

The dominant source of the salts in the ocean is river runoff from weathering of the continents (see Section 5.2). Weathering occurs very slowly over millions of years, and so the dissolved elements become equally distributed in the ocean as a result of mixing. (The total time for water to circulate through the oceans is, at most, thousands of years, which is much shorter than the geologic weathering time.) However, there are significant differences in total concentration of the dissolved salts from place to place. These differences result from evaporation and from dilution by freshwater from rain and river runoff. Evaporation and dilution processes occur only at the sea surface.

Salinity was originally defined as the mass in grams of solid material in a kilogram of seawater after evaporating the water away; this is the *absolute salinity* as described in Millero et al. (2008). For example, the average salinity of ocean water is about 35 grams of salts per kilogram of seawater (g/kg), written as "S = 35 ‰" or as "S = 35 ppt" and read as "thirty-five parts per thousand." Because evaporation measurements are cumbersome, this definition was quickly superseded in practice. In the late 1800s, Forch, Knudsen, and Sorensen (1902) introduced a more chemically based definition: "Salinity is the total amount of solid materials in grams contained in one kilogram of seawater when all the carbonate has been converted to oxide, the bromine and iodine replaced by chlorine, and all organic matter completely oxidized."

This chemical determination of salinity was also difficult to carry out routinely. The method used throughout most of the twentieth century was to determine the amount of chlorine ion (plus the chlorine equivalent of the bromine and iodine) referred to as *chlorinity*, by titration

with silver nitrate, and then to calculate salinity by a relation based on the measured ratio of chlorinity to total dissolved substances. (See Wallace, 1974, Wilson, 1975, or Millero et al., 2008 for a full account.) The current definition of salinity, denoted by S ‰, is "the mass of silver required to precipitate completely the halogens in 0.3285234 kg of the seawater sample." The current relation between salinity and chlorinity was determined in the early 1960s:

$$\text{Salinity} = 1.80655 \times \text{Chlorinity} \qquad (3.4)$$

These definitions of salinity based on chemical analyses were replaced by a definition based on seawater's electrical conductivity, which depends on salinity and temperature (see Lewis & Perkin, 1978; Lewis & Fofonoff, 1979; Figure 3.3). This conductivity-based quantity is called *practical salinity*, sometimes using the symbol psu for *practical salinity units*, although the preferred international convention has been to use no units for salinity. Salinity is now written as, say, S = 35.00 or S = 35.00 psu. The algorithm that is widely used to calculate salinity from conductivity and temperature is called the practical salinity scale 1978 (PSS 78). Electrical conductivity methods were first introduced in the 1930s (see Sverdrup, Johnson, & Fleming, 1942 for a review). Electrical conductivity depends strongly on temperature, but with a small residual due to the ion content or salinity. Therefore temperature must be controlled or measured very accurately during the conductivity measurement to determine the practical salinity. Advances in the electrical circuits and sensor systems permitted accurate compensation for temperature, making conductivity-based salinity measurements feasible (see supplemental materials in Chapter S6, Section S6.4.3 on the textbook Web site).

Standard seawater solutions of accurately known salinity and conductivity are required for accurate salinity measurement. The practical salinity (S_P) of a seawater sample is now given in terms of the ratio of the electrical conductivity of the sample at 15°C and a pressure of one standard atmosphere to that of a potassium chloride solution in which the mass fraction of KCl is 32.4356×10^{-3} at the same temperature and pressure. The potassium chloride solutions used as standards are now prepared in a single laboratory in the UK. PSS 78 is valid for the range S = 2 to 42, T = −2.0 to 35.0°C and pressures equivalent to depths from 0 to 10,000 m.

The accuracy of salinity determined from conductivity is ±0.001 if temperature is very accurately measured and standard seawater is used for calibration. This is a major improvement on the accuracy of the older titration method, which was about ±0.02. In archived data sets, salinities that are reported to three decimal places of accuracy are derived from conductivity, while those reported to two places are from titration and usually predate 1960.

The conversion from conductivity ratio to practical salinity is carried out using a computer subroutine based on the formula from Lewis (1980). The subroutine is part of the UNESCO (1983) routines for seawater calculations.

In the 1960s, the pairing of conductivity sensors with accurate thermistors made it possible to collect continuous profiles of salinity in the ocean. Because the geometry of the conductivity sensors used on these instruments change with pressure and temperature, calibration with water samples collected at the same time is required to achieve the highest possible accuracies of 0.001.

An example of the relationship between conductivity, temperature, and salinity profiles in the northeastern North Pacific is shown in Figure 3.3. Deriving salinity from conductivity requires accurate temperature measurement because the conductivity profile closely tracks temperature.

The concept of salinity assumes negligible variations in the composition of seawater. However, a study of chlorinity, density relative to pure water, and conductivity of seawater

carried out in England on samples from the world oceans (Cox, McCartney, & Culkin, 1970) revealed that the ionic composition of seawater does exhibit small variations from place to place and from the surface to deep water. It was found that the relationship between density and conductivity was a little closer than between density and chlorinity. This means that the proportion of one ion to another may change; that is, the chemical composition may change, but as long as the total weight of dissolved substances is the same, the conductivity and the density will be unchanged.

Moreover, there are geographic variations in the dissolved substances not measured by the conductivity method that affect seawater density and hence should be included in absolute salinity. The geostrophic currents computed locally from density (Section 7.6.2), based on the use of salinity PSS 78, are highly accurate. However, it is common practice to map properties on surfaces of constant potential density or related surfaces that are closest to isentropic (Section 3.5). On a global scale, these dissolved constituents can affect the definition of these surfaces.

The definition of salinity is therefore undergoing another change equivalent to that of 1978. The *absolute salinity* recommended by the IOC, SCOR, and IAPSO (2010) is a return to the original definition of "salinity," which is required for the most accurate calculation of density; that is, the ratio of the mass of all dissolved substances in seawater to the mass of the seawater, expressed in either kg/kg or g/kg (Millero et al., 2008). The new estimate for absolute salinity incorporates two corrections over PSS 78: (1) representation of improved information about the composition of the Atlantic surface seawater used to define PSS 78 and incorporation of 2005 atomic weights, and (2) corrections for the geographic dependence of the dissolved matter that is not sensed by conductivity. To maintain a consistent global salinity data set, the IOC, SCOR, and IAPSO (2010) manual strongly recommends that observations continue to be made based on conductivity and PSS 78, and reported to national archives in those practical salinity units. For calculations involving salinity, the manual indicates two corrections for calculating the absolute salinity S_A from the practical salinity S_P:

$$S_A = S_R + \delta S_A = (35.16504 \text{g kg}^{-1}/35) S_P + \delta S_A \tag{3.5}$$

The factor multiplying S_P yields the "reference salinity" S_R, which is presently the most accurate estimate of the absolute salinity of reference Atlantic surface seawater. A geographically dependent anomaly, δS_A, is then added that corrects for the dissolved substances that do not affect conductivity; this correction, as currently implemented, depends on dissolved silica, nitrate, and alkalinity. The mean absolute value of the correction globally is 0.0107 g/kg, and it ranges up to 0.025 g/kg in the northern North Pacific, so it is significant. If nutrients and carbon parameters are not measured along with salinity (which is by far the most common circumstance), then a geographic lookup table based on archived measurements is used to estimate the anomaly (McDougall, Jackett, & Millero, 2010). It is understood that the estimate (Eq. 3.5) of absolute salinity could evolve as additional measurements are made.

All of the work that appears in this book predates the adoption of the new salinity scale, and all salinities are reported as PSS 78 and all densities are calculated according to the 1980 equation of state using PSS 78.

3.5. DENSITY OF SEAWATER

Seawater density is important because it determines the depth to which a water parcel will settle in equilibrium — the least dense on top and the densest at the bottom. The distribution of density is also related to the large-scale

circulation of the oceans through the geostrophic/thermal wind relationship (see Chapter 7). Mixing is most efficient between waters of the same density because adiabatic stirring, which precedes mixing, conserves potential temperature and salinity and consequently, density. More energy is required to mix through stratification. Thus, property distributions in the ocean are effectively depicted by maps on density (*isopycnal*) surfaces, when properly constructed to be closest to isentropic. (See the discussion of potential and neutral density in Section 3.5.4.)

Density, usually denoted ρ, is the amount of mass per unit volume and is expressed in kilograms per cubic meter (kg/m^3). A directly related quantity is the specific volume anomaly, usually denoted α, where $\alpha = 1/\rho$. The density of pure water, with no salt, at 0°C, is 1000 kg/m^3 at atmospheric pressure. In the open ocean, density ranges from about 1021 kg/m^3 (at the sea surface) to about 1070 kg/m^3 (at a pressure of 10,000 dbar). As a matter of convenience, it is usual in oceanography to leave out the first two digits and use the quantity

$$\sigma_{stp} = \rho(S, T, p) - 1000\ kg/m^3 \qquad (3.6)$$

where S = salinity, T = temperature (°C), and p = pressure. This is referred to as the in situ density. In earlier literature, $\sigma_{s,t,0}$ was commonly used, abbreviated as σ_t. σ_t is the density of the water sample when the total pressure on it has been reduced to atmospheric (i.e., the water pressure p = 0 dbar) but the salinity and temperature are as measured. Unless the analysis is limited to the sea surface, σ_t is not the best quantity to calculate. If there is range of pressures, the effects of adiabatic compression should be included when comparing water parcels. A more appropriate quantity is *potential density*, which is the same as σ_t but with temperature replaced by potential temperature and pressure replaced by a single reference pressure that is not necessarily 0 dbar. Potential density is described in Section 3.5.2.

The relationship between the density of seawater and temperature, salinity, and pressure is the equation of state for seawater. The equation of state

$$\rho(S, T, p) = \rho(S, T, 0)/[1 - p/K(S, T, p)] \qquad (3.7)$$

was determined through meticulous laboratory measurements at atmospheric pressure. The polynomial expressions for the equation of state $\rho(S, T, 0)$ and the bulk modulus $K(S, T, p)$ contain 15 and 27 terms, respectively. The pressure dependence enters through the bulk modulus. The largest terms are those that are linear in S, T, and p, with smaller terms that are proportional to all of the different products of these. Thus, the equation of state is weakly nonlinear.

Today, the most common version of Eq. (3.7) is "EOS 80" (Millero & Poisson, 1980; Fofonoff, 1985). EOS 80 uses the practical salinity scale PSS 78 (Section 3.4). The formulae may be found in UNESCO (1983), which provides practical computer subroutines and are included in various texts such as Pond and Pickard (1983) and Gill (1982). EOS 80 is valid for T = −2 to 40°C, S = 0 to 40, and pressures from 0 to 10,000 dbar, and is accurate to 9×10^{-3} kg/m^3 or better. A new version of the equation of state has been introduced (IOC, SCOR, and IAPSO, 2010), based on a new definition of salinity and is termed TEOS-10. Only EOS 80 is used in this book.

Historically, density was calculated from tables giving the dependence of the density on salinity, temperature, and pressure. Earlier determinations of density were based on measurements by Forch, Jacobsen, Knudsen, and Sorensen and were presented in the Hydrographical Tables (Knudsen, 1901). Cox et al. (1970) found that the σ_0 values (at T = 0°C) in "Knudsen's Tables" were low by about 0.01 (on average) in the salinity range from 15 − 40, and by up to 0.06 at lower salinities and temperatures.

To determine seawater density over a range of salinities in the laboratory, Millero (1967) used a magnetic float densimeter. A Pyrex glass float containing a permanent magnet floats in a

250 ml cell that contains the seawater and is surrounded by a solenoid, with the entire apparatus sitting in a constant temperature bath. The float is slightly less dense than the densest seawater and is loaded with small platinum weights until it just sinks to the bottom of the cell. A current through the solenoid is then slowly increased until the float just lifts off the bottom of the cell. The density of the seawater is then related to the current through the solenoid. The relation between current and density is determined by carrying out a similar experiment with pure water in the cell. The accuracy of the relative density determined this way is claimed to be $\pm 2 \times 10^{-6}$ (at atmospheric pressure). But as the absolute density of pure water is known to be only $\pm 4 \times 10^{-6}$, the actual accuracy of seawater density is more limited. The influence of pressure was determined using a high pressure version of the previously mentioned densimeter to measure the bulk modulus (K). K has also been determined from measurements of sound speed in seawater because sound speed depends on the bulk modulus and seawater compressibility.

The following subsections explore how seawater density depends on temperature, salinity, and pressure, and discusses concepts (such as potential and neutral density) that reduce, as much as possible, the effects of compressibility on a given analysis.

3.5.1. Effects of Temperature and Salinity on Density

Density values evaluated at the ocean's surface pressure are shown in Figure 3.1 (curved contours) for the whole range of salinities and temperatures found anywhere in the oceans. The shaded bar in the figure shows that most of the ocean lies within a relatively narrow salinity range. More extreme values occur only at or near the sea surface, with fresher waters outside this range (mainly in areas of runoff or ice melt) and the most saline waters in relatively confined areas of high evaporation (such as marginal seas). The ocean's temperature range produces more of the ocean's density variation than does its salinity range. In other words, temperature dominates oceanic density variations for the most part. (As noted previously, an important exception is where surface waters are relatively fresh due to large precipitation or ice melt; that is, at high latitudes and also in the tropics beneath the rainy Intertropical Convergence Zone of the atmosphere.) The curvature of the density contours in Figure 3.1 is due to the nonlinearity of the equation of state. The curvature means that the density change for a given temperature or salinity change is different at different temperatures or salinities.

To emphasize this point, Table 3.2 shows the change of density ($\Delta\sigma_t$) for a temperature change (ΔT) of $+1$ K (left columns) and the value of $\Delta\sigma_t$ for a salinity change (ΔS) of $+0.5$ (right columns). These are arbitrary choices for changes in temperature and salinity. The most important thing to notice in the table is how density varies at different temperatures and salinities for given changes in each. At high temperatures, σ_t varies significantly with T at all salinities. As temperature decreases, the rate of variation with T decreases, particularly at low salinities (as found at high latitudes or in estuaries). The change of σ_t with ΔS is about the same at all temperatures and salinities, but is slightly greater at low temperature.

3.5.2. Effect of Pressure on Density: Potential Density

Seawater is compressible, although not nearly as compressible as a gas. As a water parcel is compressed, the molecules are pushed closer together and the density increases. At the same time, and for a completely different physical reason, adiabatic compression causes the temperature to increase, which slightly offsets the density increase due to compression. (See discussion of potential temperature in Section 3.3.)

TABLE 3.2 Variation of Density ($\Delta\sigma_t$) with Variations of Temperature (ΔT) and of Salinity (ΔS) as Functions of Temperature and Salinity

Salinity	0	20	35	40	0	20	35	40
Temperature (°C)	$\Delta\sigma_t$ for $\Delta T = +1°C$				$\Delta\sigma_t$ for $\Delta S = +0.5$			
30	−0.31	−0.33	−0.34	−0.35	0.38	0.37	0.37	0.38
20	−0.21	−0.24	−0.27	−0.27	0.38	0.38	0.38	0.38
10	−0.09	−0.14	−0.18	−0.18	0.39	0.39	0.39	0.39
0	+0.06	−0.01	−0.06	−0.07	0.41	0.40	0.40	0.40

Density is primarily a function of pressure (Figure 3.4) because of this compressibility. Pressure effects on density have little to do with the initial temperature and salinity of the water parcel. To trace a water parcel from one place to another, the dependence of density on pressure should be removed. An early attempt was to use σ_t, defined earlier, in which the pressure effect was removed from density but not from temperature. It is now standard practice to use *potential density*, in which density is calculated using potential temperature instead of temperature. (The measured salinity is used.) Potential density is the density that a parcel would have if it were moved adiabatically to a chosen reference pressure. If the reference pressure is the sea surface, then we first compute the potential temperature of the parcel relative to surface pressure, then evaluate the density at pressure 0 dbar.[1] We refer to potential density referenced to the sea surface (0 dbar) as σ_θ, which signifies that potential temperature and surface pressure have been used.

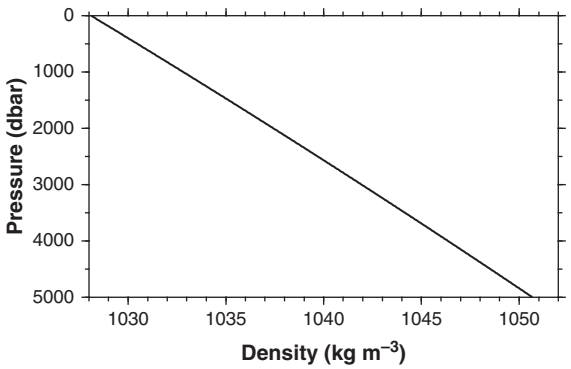

FIGURE 3.4 Increase in density with pressure for a water parcel of temperature 0°C and salinity 35.0 at the sea surface.

The reference pressure for potential density can be any pressure, not just the pressure at the sea surface. For these potential densities, potential temperature is calculated relative to the chosen reference pressure and then the potential density is calculated relative to the same reference pressure. It is common to refer to potential density referenced to 1000 dbar as σ_1, referenced to 2000 dbar as σ_2, to 3000 dbar as σ_3 and so on, following Lynn and Reid (1968).

3.5.3. Specific Volume and Specific Volume Anomaly

The specific volume (α) is the reciprocal of density so it has units of m^3/kg. For some purposes it is more useful than density. The in situ specific volume is written as $\alpha_{s,t,p}$. The

[1] The actual pressure at the sea surface is the atmospheric pressure, but we do not include atmospheric pressure in many applications since pressure ranges within the ocean are so much larger.

specific volume anomaly (δ) is also sometimes convenient. It is defined as:

$$\delta = \alpha_{s,t,p} - \alpha_{35,0,p} \tag{3.8}$$

The anomaly is calculated relative to $\alpha_{35,0,p}$, which is the specific volume of seawater of salinity 35 and temperature 0°C at pressure p. With this standard δ is usually positive. The equation of state relates α (and δ) to salinity, temperature, and pressure. Originally all calculations of geostrophic currents from the distribution of mass were done by hand using tabulations of the component terms of δ, described in previous editions of this book. With modern computer methods, tabulations are not necessary. The computer algorithms for dynamic calculations (Section 7.5.1) still use specific volume anomaly δ, computed using subroutines, rather than the actual density ρ, to increase the calculation precision.

3.5.4. Effect of Temperature and Salinity on Compressibility: Isentropic Surfaces and Neutral Density

Cold water is more compressible than warm water; it is easier to deform a cold parcel than a warm parcel. When two water parcels with the same density but different temperature and salinity characteristics (one warm/salty, the other cold/fresh) are submerged to the same pressure, the colder parcel will be denser. If there were no salt in seawater, so that density depended only on temperature and pressure, then potential density as defined earlier, using any single pressure for a reference, would be adequate for defining a unique *isentropic surface*. An isentropic surface is one along which water parcels can move adiabatically, that is, without external input of heat or salt.

When analyzing properties within the ocean to determine where water parcels originate, it is assumed that motion and mixing is mostly along a quasi-isentropic surface and that mixing across such a surface (quasi-vertical mixing) is much less important (Montgomery, 1938). However, because seawater density depends on both salinity and temperature, the actual surface that a water parcel moves along in the absence of external sources of heat or freshwater depends on how the parcel mixes along that surface since its temperature and salinity will be altered as it mixes with adjacent water parcels on that surface. This quasi-lateral mixing alters the temperature (and salinity) and therefore, the compressibility of the mixture. As a result, when it moves laterally, the parcel will equilibrate at a different pressure than if there had been no mixing. This means that there are no closed, unique isentropic surfaces in the ocean, since if our water parcel were to return to its original latitude and longitude, it will have moved to a different density and hence pressure because its temperature and salinity will have changed due to mixing along that surface. Note that these effects are important even without diapycnal mixing between water parcels on different isentropic surfaces (quasi-vertical mixing), which also can change temperature, salinity, and compressibility.

The density differences associated with these differences in compressibility can be substantial (Figure 3.5). For instance, water spilling out of the Mediterranean Sea through the Strait of Gibraltar is saline and rather warm compared with water spilling into the Atlantic from the Nordic Seas over the Greenland-Iceland ridge (Chapter 9). The Mediterranean Water (MW) density is actually higher than the Nordic Sea Overflow Water (NSOW) density where they flow over their respective sills, which are at about the same depth. However, the warm, saline MW (13.4°C, 37.8 psu) is not as compressible as the much colder NSOW (about 1°C, 34.9 psu; Price & Baringer, 1994). The potential density relative to 4000 dbar of MW is lower than that of the more compressible NSOW. The NSOW reaches the bottom of the North Atlantic, while the MW does not. (As both types of water plunge

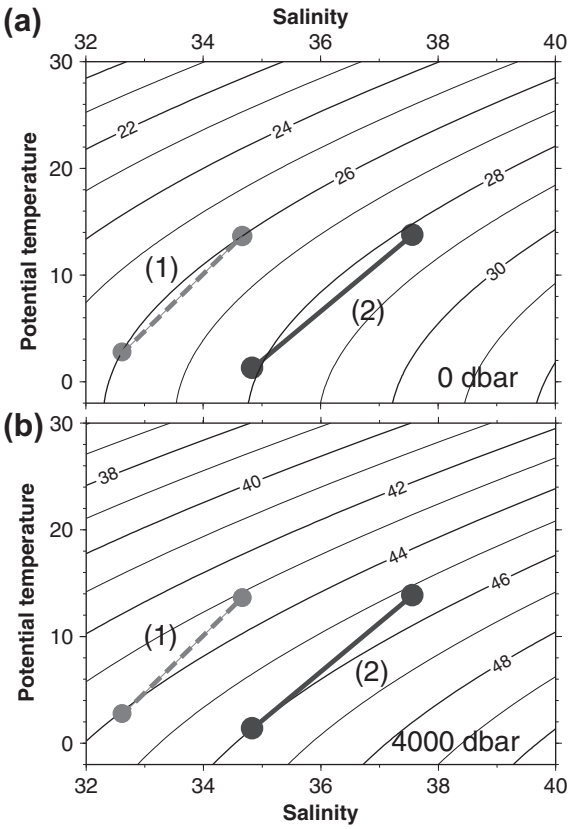

FIGURE 3.5 Potential density relative to (a) 0 dbar and (b) 4000 dbar as a function of potential temperature (relative to 0 dbar) and salinity. Parcels labeled 1 have the same density at the sea surface. The parcels labeled 2 represents Mediterranean (saltier) and Nordic Seas (fresher) source waters at their sills.

downward, they entrain or mix with the waters that they pass through. This also has an effect on how deep they fall, so the difference in compressibility is not the only cause for different outcomes.)

Restating this more generally, changing the reference pressure for potential density alters the density difference between two water parcels (Figure 3.5). For the pair labeled 1, the densities are the same at the sea surface (upper panel). Because the cold parcel compresses more than the warm one with increasing pressure, the cold parcel is denser than the warm one at higher pressure (lower panel). The pair labeled 2 illustrates the MW (warm, salty) and NSOW (cold, fresh) pair with their properties at the sills where they enter the North Atlantic. At the sea surface, which neither parcel ever reaches, the Mediterranean parcel would actually be denser than the Nordic Seas parcel. Near the ocean bottom, represented by 4000 dbar (Figure 3.5b), the colder Nordic Seas parcel is markedly denser than the Mediterranean parcel. Therefore, if both parcels dropped to the ocean bottom from their respective sills, without any mixing, the Nordic Seas parcel would lie under the Mediterranean parcel. (In actuality, as already mentioned, there is a large amount of entrainment mixing as these parcels drop down into the North Atlantic.)

The surfaces that we use to map and trace water parcels should approximate isentropic surfaces. Early choices, that were an improvement over constant depth surfaces, included sigma-t surfaces (Montgomery, 1938) and even potential temperature surfaces (Worthington and Wright, 1970). A method, introduced by Lynn and Reid (1968), that produces surfaces that are closer to isentropic uses isopycnals with a reference pressure for the potential density that is within 500 m of the pressure of interest. Therefore when working in the top 500 m, a surface reference pressure is used. When working at 500 to 1500 m, a reference pressure of 1000 dbar is used, and so forth. Experience has shown this pressure discretization is sufficient to remove most of the problems associated with the effect of pressure on density. When isopycnals mapped in this fashion move into a different pressure range, they must be patched onto densities at the reference pressure in the new range. Reid (1989, 1994, 1997, 2003) followed this practice in his monographs on Pacific, Atlantic, and Indian Ocean circulations.

It is less complicated to use a continuously varying surface rather than one patched from different reference pressures, although in practice there is little difference between them.

"Neutral surfaces," introduced by Ivers (1975), a student working with J.L. Reid, use a nearly continuously varying reference pressure. If a parcel is followed along its path from one observation station to the next, assuming the path is known, then it is possible to track its pressure and adjust its reference pressure and density at each station. McDougall (1987a) refined this neutral surface concept and introduced it widely. Jackett and McDougall (1997) created a computer program for computing their version of this *neutral density*, based on a standard climatology (average temperature and salinity on a grid for the whole globe, derived from all available observations; Section 6.6.2), marching away from a single location in the middle of the Pacific. The Jackett and McDougall neutral density is denoted γ^N with numerical values that are similar to those of potential density (with units of kg/m^3). Neutral density depends on latitude, longitude, and pressure, and is defined only for ranges of temperature and salinity that occur in the open ocean. This differs from potential density, which is defined for all values of temperature and salinity through a well-defined equation of state that has been determined in the laboratory and is independent of location. Neutral density cannot be contoured as a function of potential temperature and salinity analogously to Figure 3.5 for density or potential density.

The advantage of neutral density for mapping quasi-isentropic surfaces is that it removes the need to continuously vary the reference pressure along surfaces that have depth variation (since this is already done in an approximate manner within the provided software and database). Neutral density is a convenient tool. Both potential and neutral density surfaces are approximations to isentropic surfaces. Ideas and literature on how to best approximate isentropic surfaces continue to be developed; neutral density is currently the most popular and commonly used approximation for mapping isentropes over large distances that include vertical excursions of more than several hundred meters.

3.5.5. Linearity and Nonlinearity in the Equation of State

As described earlier, the equation of state (3.6) is somewhat nonlinear in temperature, salinity, and pressure; that is, it includes products of salinity, temperature, and pressure. For practical purposes, in theoretical and simple numerical models, the equation of state is sometimes approximated as linear and its pressure dependence is ignored:

$$\rho \approx \rho_0 + \alpha(T - T_0) + \beta(S - S_0); \quad \alpha = \partial\rho/\partial T \text{ and } \beta = \partial\rho/\partial S \tag{3.9}$$

where ρ_0, T_0, and S_0 are arbitrary constant values of ρ, T, and S; they are usually chosen as the mean values for the region being modeled. Here α is the *thermal expansion coefficient*, which expresses the change in density for a given change in temperature (and should not be confused with specific volume, defined with the same symbol in Section 3.5.3), and β is the *haline contraction coefficient*, which is the change in density for a given change in salinity. The terms α and β are nonlinear functions of salinity, temperature, and pressure; their mean values are chosen for linear models. Full tables of values are given in UNESCO (1987). The value of $\alpha\rho$ (at the sea surface and at a salinity of 35 psu) ranges from $53 \times 10^{-6}\,K^{-1}$ at a temperature of 0°C to $257 \times 10^{-6}\,K^{-1}$ at a temperature of 20°C. The value of $\beta\rho$ (at the sea surface and at a salinity of 35 psu) ranges from $785 \times 10^{-6}\,psu^{-1}$ (at a temperature of 0°C) to $744 \times 10^{-6}\,psu^{-1}$ (at a temperature of 20°C).

Nonlinearity in the equation of state leads to the curvature of the density contours in Figures 3.1 and 3.5. Mixing between two water parcels must occur along straight lines in the temperature/salinity planes of Figures 3.1 and 3.5. Because of the concave curvature of the density

contours, when two parcels of the same density but different temperature and salinity are mixed together, the mixture has higher density than the original water parcels. Thus the concavity of the density contours means that there is a contraction in volume as water parcels mix. This effect is called *cabbeling* (Witte, 1902). In practice, cabbeling may be of limited importance, having demonstrable importance only where water parcels of very different initial properties mix together. Examples of problems where cabbeling has been a factor are in the formation of dense water in the Antarctic (Foster, 1972) and in the modification of intermediate water in the North Pacific (Talley & Yun, 2001).

There are two other important mixing effects associated with the physical properties of seawater: thermobaricity and double diffusion. *Thermobaricity* (McDougall, 1987b) is best explained by the rotation with depth of potential density contours in the potential temperature–salinity plane (Section 3.5.4). As in Figure 3.5, consider two water parcels of different potential temperature and salinity in which the warmer, saltier parcel is slightly denser than the colder, fresher one. (This is a common occurrence in subpolar regions such as the Arctic and the Antarctic.) If these two water parcels are suddenly brought to a greater pressure, it is possible for them to reverse their relative stratification, with the colder, fresher one compressing more than the warmer one, and therefore becoming the denser of the two parcels. The parcels would now be vertically stable if the colder, fresher one were beneath the warmer, saltier one. Thermobaricity is an important effect in the Arctic, defining the relative vertical juxtaposition of the Canadian and Eurasian Basin Deep Waters (Section 12.2).

Double diffusion results from a difference in diffusivities for heat and salt, therefore, it is not a matter of linearity or nonlinearity. At the molecular level, these diffusivities clearly differ. Because double diffusive effects are apparent in the ocean's temperature–salinity properties, the difference in diffusivities scales up in some way to the eddy diffusivity. Diffusivity and mixing are discussed in Chapter 7, and double diffusion in Section 7.4.3.2.

3.5.6. Static Stability and Brunt-Väisälä Frequency

Static stability, denoted by E, is a formal measure of the tendency of a water column to overturn. It is related to the density stratification, with higher stability where the water column is more stratified. A water column is statically stable if a parcel of water that is moved adiabatically (with no heat or salt exchange) up or down a short distance returns to its original position. The vigor with which the parcel returns to its original position depends on the density difference between the parcel and the surrounding water column at the displaced position. Therefore the rate of change of density of the water column with depth determines a water column's static stability. The actual density of the parcel increases or decreases as it is moved down or up because the pressure on it increases or decreases, respectively. This adiabatic change in density must be accounted for in the definition of static stability.

The mathematical derivation of the static stability of a water column is presented in detail in Pond and Pickard (1983) and other texts. The full expression for E is complicated. For very small vertical displacements, static stability might be approximated as

$$E \approx -(1/\rho)\ (\partial\rho/\partial z) \qquad (3.10a)$$

where ρ is in situ density. The water column is stable, neutral, or unstable depending on whether E is positive, zero, or negative, respectively. Thus, if the density gradient is positive downwards, the water column is stable and there is no tendency for vertical overturn.

For larger vertical displacements, a much better approximation uses local potential density, σ_n:

$$E = -(1/\rho)(\partial\sigma_n/\partial z) \qquad (3.10b)$$

Here the potential density anomaly σ_n is computed relative to the pressure at the center of the interval used to compute the vertical gradient. This local pressure reference approximately removes the adiabatic pressure effect. Many computer subroutines for seawater properties use this standard definition. An equivalent expression for stability is

$$E = -(1/\rho)(\partial\rho/\partial z) - (g/C^2) \qquad (3.10c)$$

where ρ is in situ density, g = acceleration due to gravity, and C = in situ sound speed. The addition of the term g/C^2 allows for the compressibility of seawater. (Sound waves are compression waves; Section 3.7.)

A typical density profile from top to bottom of the ocean has a surface mixed layer with low stratification, an upper ocean layer with an intermediate amount of stratification, an intermediate layer of high stratification (*pycnocline*), and a deep layer of low stratification (Section 4.2). The water in the pycnocline is very stable; it takes much more energy to displace a particle of water up or down than in a region of lesser stability. Therefore turbulence, which causes most of the mixing between different water bodies, is less able to penetrate through the stable pycnocline than through less stable layers. Consequently, the pycnocline is a barrier to the vertical transport of water and water properties. The stability of these layers is measured by E. In the upper 1000 m in the open ocean, values of E range from 1000×10^{-8} m^{-1} to 100×10^{-8} m^{-1}, with larger values in the pycnocline. Below 1000 m, E decreases; in abyssal trenches E may be as low as 1×10^{-8} m^{-1}.

Static instabilities may be found near the interfaces between different waters in the process of mixing. Because these instabilities occur at a small vertical scale, on the order of meters, they require continuous profilers for detection. Unstable conditions with vertical extents greater than tens of meters are uncommon below the surface layer.

The *buoyancy* (*Brunt-Väisälä*) *frequency* associated with internal gravity waves (Chapter 8) is an intrinsic frequency associated with static stability. If a water parcel is displaced upward in a statically stable water column, it will sink and overshoot the original position. The denser water beneath its original position will force it back up into lighter water, and it will continue oscillating. The frequency of the oscillation depends on the static stability: the more stratified the water column, the higher the static stability and the higher the buoyancy frequency. The Brunt-Väisälä frequency, N, is an intrinsic frequency of internal waves:

$$N^2 = gE \approx g[-(1/\rho)(\partial\sigma_n/\partial z)] \qquad (3.11)$$

The frequency in cycles/sec (hertz) is $f = N/2\pi$ and the period is $\tau = 2\pi/N$. In the upper ocean, where E typically ranges from 1000×10^{-8} to 100×10^{-8} m^{-1}, periods are $\tau = 10$ to 33 min (Figure 3.6). For the deep ocean, $E = 1 \times 10^{-8}$ m^{-1} and $\tau \approx 6$ h.

The final quantity that we define based on vertical density stratification is the "stretching" part of the *potential vorticity* (Section 7.6). Potential vorticity is a dynamical property of a fluid analogous to angular momentum. Potential vorticity has three parts: rotation due to Earth's rotation (planetary vorticity), rotation due to relative motions in the fluid (relative vorticity, for instance, in an eddy), and a stretching component proportional to the vertical change in density, which is analogous to layer thickness (Eq. 7.41). In regions where currents are weak, relative vorticity is small and the potential vorticity can be approximated as

$$Q \approx -(f/\rho)(\partial\rho/\partial z) \qquad (3.12a)$$

This is sometimes called "isopycnic potential vorticity." The vertical density derivative is

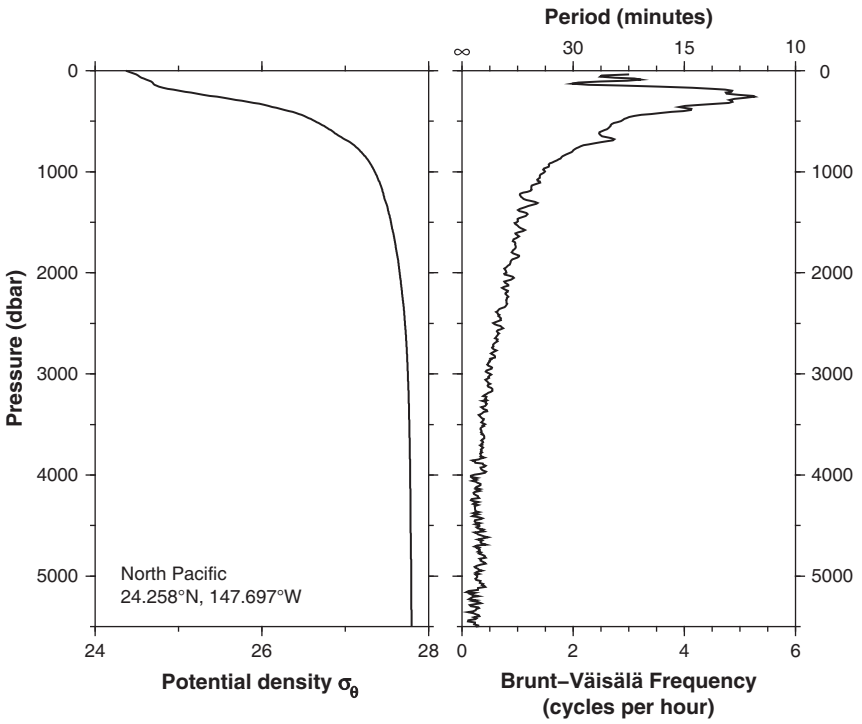

FIGURE 3.6 (a) Potential density and (b) Brunt-Väisälä frequency (cycles/h) and period (minutes) for a profile in the western North Pacific.

calculated from locally referenced potential density, so it can be expressed in terms of Brunt-Väisälä frequency:

$$Q = (f/g)N^2 \qquad (3.12b)$$

3.5.7. Freezing Point of Seawater

The salt in seawater depresses the freezing point below 0°C (Figure 3.1). An algorithm for calculating the freezing point of seawater is given by Millero (1978). Depression of the freezing point is why a mixture of salt water and ice is used to make ice cream; as the ice melts, it cools the water (and ice cream) below 0°C. At low salinities, below the salinity of most seawater, cooling water reaches its maximum density before freezing and sinks while still fluid. The water column then overturns and mixes until the whole water column reaches the temperature of maximum density. On further cooling the surface water becomes lighter and the overturning stops. The water column freezes from the surface down, with the deeper water remaining unfrozen. However, at salinities greater than 24.7 psu, maximum density is achieved at the freezing point. Therefore more of the water column must be cooled before freezing can begin, so freezing is delayed compared with the freshwater case.

3.6. TRACERS

Dissolved matter in seawater can help in tracing specific water masses and pathways of flow. Some of these properties can be used for dating seawater (determine the length of time since the water was last at the sea surface; Section 4.7). Most of these constituents occur in such small concentrations that their variations

do not significantly affect density variations or the relationship between chlorinity, salinity, and conductivity. (See Section 3.5 for comments on this.) These additional properties of seawater can be: conservative or non-conservative; natural or anthropogenic (man-made); stable or radioactive; transient or non-transient. The text by Broecker and Peng (1982) describes the sources and chemistry of many tracers in detail.

For a tracer to be *conservative* there are no significant processes other than mixing by which the tracer is changed below the surface. Even salinity, potential temperature, and hence density, can be used as conservative tracers since they have extremely weak sources within the ocean. This near absence of in situ sources and sinks means that the spreading of water masses in the ocean can be approximately traced from their origin at the sea surface by their characteristic temperature/salinity values. Near the surface, evaporation, precipitation, runoff, and ice processes change salinity, and many surface heat-transfer processes change the temperature (Section 5.4). Absolute salinity can be changed only very slightly within the ocean due to changes in dissolved nutrients and carbon (end of Section 3.4). Temperature can be raised very slightly by geothermal heating at the ocean bottom. Even though water coming out of bottom vents at some mid-ocean ridges can be extremely hot (up to 400°C), the total amount of water streaming out of the vents is tiny, and the high temperature quickly mixes away, leaving a miniscule large-scale temperature increase.

Non-conservative properties are changed by chemical reactions or biological processes within the water column. Dissolved oxygen is an example. Oxygen enters the ocean from the atmosphere at the sea surface. It is also produced through photosynthesis by phytoplankton in the sunlit upper ocean (photic zone or euphotic zone) and consumed by respiration by zooplankton, bacteria, and other creatures. Equilibration with the atmosphere keeps ocean mixed layer waters at close to 100% saturation. Below the surface layer, oxygen content drops rapidly. This is not a function of the temperature of the water, which generally is lower at depth, since cold water can hold *more* dissolved oxygen than warm water. (For example, for a salinity of 35: at 30°C, 100% oxygen saturation occurs at 190 μmol/kg; at 10°C it is 275 μmol/kg; and at 0°C it is 350 μmol/kg.) The drop in oxygen content and saturation with depth is due to respiration within the water column, mainly by bacteria feeding on organic matter (mostly dead plankton and fecal pellets) sinking from the photic zone. Since there is no source of oxygen below the mixed layer and photic zone, oxygen decreases with increasing age of the subsurface water parcels. Oxygen is also used by nitrifying bacteria, which convert the nitrogen in ammonium (NH_4) to nitrate (NO_3).

The rate at which oxygen is consumed is called the *oxygen utilization rate*. This rate depends on local biological productivity so it is not uniform in space. Therefore the decrease in oxygen from a saturated surface value is not a perfect indication of age of the water parcel, especially in the biologically active upper ocean and continental shelves. However, below the thermocline, the utilization rate is more uniform and changes in oxygen following a water parcel correspond relatively well to age.

Nutrients are another set of natural, non-conservative, commonly observed properties. These include dissolved silica, phosphate, and the nitrogen compounds (ammonium, nitrite, and nitrate). Nutrients are essential to ocean life so they are consumed in the ocean's surface layer where life is abundant; consequently, concentrations there are low. Nutrient content increases with depth and age, as almost a mirror image of the oxygen decrease. Silica is used by some organisms to form protective shells. Silica re-enters the water column when the hard parts of these organisms dissolve as they fall to the ocean floor. Some of this material reaches the

seafloor and accumulates, creating a silica source on the ocean bottom as well. Some silica also enters the water column through venting at mid-ocean ridges. The other nutrients (nitrate, nitrite, ammonium, and phosphate) re-enter the water column as biological (bacterial) activity decays the soft parts of the falling detritus. Ammonium and phosphate are immediate products of the decay. Nitrifying bacteria, which are present through the water column, then convert ammonium to nitrite and finally nitrate; this process also, in addition to respiration, consumes oxygen. Because oxygen is consumed and nutrients are produced, the ratios of nitrate to oxygen and of phosphate to oxygen are nearly constant throughout the oceans. These proportions are known as "Redfield ratios," after Redfield (1934) who demonstrated the near-constancy of these proportions. Nutrients are discussed further in Section 4.6.

Other non-conservative properties related to the ocean's carbon system, including dissolved inorganic carbon, dissolved organic carbon, alkalinity, and pH, have been widely measured over the past several decades. These have both natural and anthropogenic sources and are useful tracers of water masses.

Isotopes that occur in trace quantities are also useful. Two have been widely measured: ^{14}C and ^{3}He. ^{14}C is radioactive and non-conservative. ^{3}He is conservative. Both have predominantly natural sources but both also have anthropogenic sources in the upper ocean. Isotope concentrations are usually measured and reported in terms of ratios to the more abundant isotopes. For ^{14}C, the reported unit is based on the ratio of ^{14}C to ^{12}C. For ^{3}He, the reported unit is based on the ratio of ^{3}He to ^{4}He. Moreover, the values are often reported in terms of the normalized difference between this ratio and a standard value, usually taken to be the average atmospheric value (see Broecker & Peng, 1982).

Most of the ^{14}C in the ocean is natural. It is created continuously in the atmosphere by cosmic ray bombardment of nitrogen, and enters the ocean through gas exchange. "Bomb" radiocarbon is an anthropogenic tracer that entered the upper ocean as a result of atomic bomb tests between 1945 and 1963 (Key, 2001). In the ocean, ^{14}C and ^{12}C are incorporated by phytoplankton in nearly the same ratio as they appear in the atmosphere. After the organic material dies and leaves the photic zone, the ^{14}C decays radioactively, with a half-life of 5730 years. The ratio of ^{14}C to ^{12}C decreases. Since values are reported as anomalies, as the difference from the atmospheric ratio, the reported oceanic quantities are generally negative (Section 4.7 and Figure 4.24). The more negative the anomaly, the older the water. Positive anomalies throughout the upper ocean originated from the anthropogenic bomb release of ^{14}C.

The natural, conservative isotope ^{3}He originates in Earth's mantle and is outgassed at vents in the ocean floor. It is usually reported in terms of its ratio to the much more abundant ^{4}He compared with this ratio in the atmosphere. It is an excellent tracer of mid-depth circulation, since its sources tend to be the tops of mid-ocean ridges, which occur at about 2000 m. The anthropogenic component of ^{3}He is described in the last paragraph of this Section.

Another conservative isotope that is often measured in seawater is the stable (heavy) isotope of oxygen, ^{18}O. Measurements are again reported relative to the most common isotope ^{16}O. Rainwater is depleted in this heavy isotope of oxygen (compared with seawater) because it is easier for the lighter, more common isotope of oxygen, ^{16}O, to evaporate from the sea and land. A second step of reduction of ^{18}O in atmospheric water vapor relative to seawater occurs when rain first forms, mostly at warmer atmospheric temperatures, since the heavier isotope falls out preferentially. Thus rainwater is depleted in ^{18}O relative to seawater, and rain formed at lower temperatures is more depleted than at higher temperatures. For physical oceanographers, ^{18}O content can be a useful indicator in a high latitude region of whether the source of

freshwater at the sea surface is rain/runoff/glacial melt (lower ^{18}O content), or melted sea ice (higher content). In paleoclimate records, it reflects the temperature of the precipitation (higher ^{18}O in warmer rain); ice formed during the (cold) glacial periods is more depleted in ^{18}O than ice formed in the warm interglacials and hence ^{18}O content is an indicator of relative global temperature.

Transient tracers are chemicals that have been introduced by human activity; hence they are anthropogenic. They are gradually invading the ocean, marking the progress of water from the surface to depth. They can be either stable or radioactive. They can be either conservative or non-conservative. Commonly measured transient tracers include chlorofluorocarbons, tritium, and much of the upper ocean ^{3}He and ^{14}C. Chlorofluorocarbons (CFCs) were introduced as refrigerants and for industrial use. They are extremely stable (conservative) in seawater. Their usage peaked in 1994, when recognition of their role in expanding the ozone hole in the atmosphere finally led to international conventions to phase out their use. Because different types of CFCs were used over the years, the ratio of different types in a water parcel can yield approximate dates for when the water was at the sea surface. Tritium is a radioactive isotope of hydrogen that has also been measured globally; it was released into the atmosphere through atomic bomb testing in the 1960s and then entered the ocean, primarily in the Northern Hemisphere. Tritium decays to ^{3}He with a half-life of 12.4 years, which is comparable to the circulation time of the upper ocean gyres. When ^{3}He is measured along with tritium, the time since the water was at the sea surface can be estimated (Jenkins, 1998).

3.7. SOUND IN THE SEA

In the atmosphere, we receive much of our information about the material world by means of wave energy, either electromagnetic (light) or mechanical (sound). In the atmosphere, light in the visible part of the spectrum is attenuated less than sound; we can see much farther away than we can hear. In the sea the reverse is true. In clear ocean water, sunlight may be detectable (with instruments) down to 1000 m, but the range at which humans can see details of objects is rarely more than 50 m, and usually less. On the other hand, sound waves can be detected over vast distances and are a much better vehicle for undersea information than light.

The ratio of the speed of sound in air to that in water is small (about 1:4.5), so only a small amount of sound energy starting in one medium can penetrate into the other. This contrasts with the relatively efficient passage of light energy through the air/water interface (speed ratio only about 1.33:1). This is why a person standing on the shore can see into the water but cannot hear any noises in the sea. Likewise, divers cannot converse underwater because their sounds are generated in the air in the throat and little of the sound energy is transmitted into the water. Sound sources used in the sea generate sound energy in solid bodies (transducers), for example, electromagnetically, in which the speed of sound is similar to that in water. Thus the two are acoustically "matched" and the transducer energy is transmitted efficiently into the sea.

Sound is a wave. All waves are characterized by amplitude, frequency, and wavelength (Section 8.2). Sound speed (C), frequency (n), and wavelength (λ) are connected by the wave equation $C = n\lambda$. The speed does not depend on frequency, so the wavelength depends on sound speed and frequency. The frequencies of sounds range from 1 Hz or less (1 Hz = 1 vibration per second) to thousands of kilohertz (1 kHz = 1000 cycles/sec). The wavelengths of sounds in the sea cover a vast range, from about 1500 m for $n = 1$ Hz to 7 cm for $n = 200$ kHz. Most underwater sound instruments use

a more restricted range from 10 to 100 kHz, for which the wavelengths are 14 to 1.4 cm.

There are many sources of sound in the sea. A hydrophone listening to the ambient sound in the sea will record a wide range of frequencies and types of sounds, from low rumbles to high-frequency hisses. Some sources of undersea sounds are microseisms (10 − 100 Hz); ships (50 − 1500 Hz); the action of wind, waves, and rain at the surface (1 − 20 kHz); cavitation of air bubbles and animal noises (10 − 400 Hz); and fish and crustaceans (1 − 10 kHz). Noises associated with sea ice range from 1 − 10 kHz.

Sound is a compressional wave; water molecules move closer together and farther apart as the wave passes. Therefore sound speed depends on the medium's compressibility. The more compressible a medium is for a given density, the slower the wave since more activity is required to move the molecules. The speed of sound waves in the sea, C, is given by

$$C = (\beta\rho)^{-1/2} \text{ where } \beta = \rho^{-1}(\partial\rho/\partial p)_{\theta,S} \tag{3.13}$$

β is the adiabatic compressibility of seawater (with potential temperature and salinity constant), ρ is the density, p is the pressure, θ is the potential temperature, and S is the salinity. Since β and ρ depend (nonlinearly) on temperature and pressure, and to a lesser extent, salinity, so does the speed of sound waves. There are various formulae for the dependence of Eq. (3.13) on T, S, and p; all derived from experimental measurements. The two most accepted are those of Del Grosso (1974) and of Chen and Millero (1977); Del Grosso's equation is apparently more accurate, based on results from acoustic tomography and inverted echo sounder experiments (e.g., Meinen & Watts, 1997). Both are long and nonlinear polynomials, as is the equation of state. We present a simpler formula, which itself is simplified from Mackenzie (1981) and is similar to Del Grosso (1974), to illustrate features of the relationship:

$$\begin{aligned} C = {} & 1448.96 + 4.59T - 0.053T^2 \\ & + 1.34(S - 35) + 0.016p \end{aligned} \tag{3.14}$$

in which T, S, and p are temperature, salinity, and depth, and the constants have the correct units to yield C in m/s. The sound speed is 1449 m/s at T = 0°C, S = 35, and p = 0. The sound speed increases by 4.5 m/s for $\Delta T = +1$ K, by 1.3 m/s for $\Delta S = +1$, and by 16 m/s for $\Delta p = 1000$ dbar.

Sound speed is higher where the medium is less compressible. Seawater is less compressible when it is warm, as noted in the previous potential density discussion and apparent from the simplified equation (3.14). Seawater is also less compressible at high pressure, where the fluid is effectively more rigid because the molecules are pushed together. Salinity variations have a negligible effect in most locations. In the upper layers, where temperature is high, sound speed is high, and decreases downward with decreasing temperature (Figure 3.7). However, pressure increases with depth, so that at middepth, the decrease in sound speed due to cooler water is overcome by an increase in sound speed due to higher pressure. In most areas of the ocean, the warm water at the surface and the high pressure at the bottom produce maximum sound speeds at the surface and bottom and a minimum in between. The sound-speed minimum is referred to as the **SO**und **F**ixing **A**nd **R**anging (SOFAR) channel. In Figure 3.6, the sound-speed minimum is at about 700 m depth. In regions where temperature is low near the sea surface, for instance at high latitudes, there is no surface maximum in sound speed, and the sound channel is found at the sea surface.

Sound propagation can be represented in terms of rays that trace the path of the sound (Figure 3.8). In the SOFAR channel, at about 1100 m in Figure 3.8, sound waves directed at

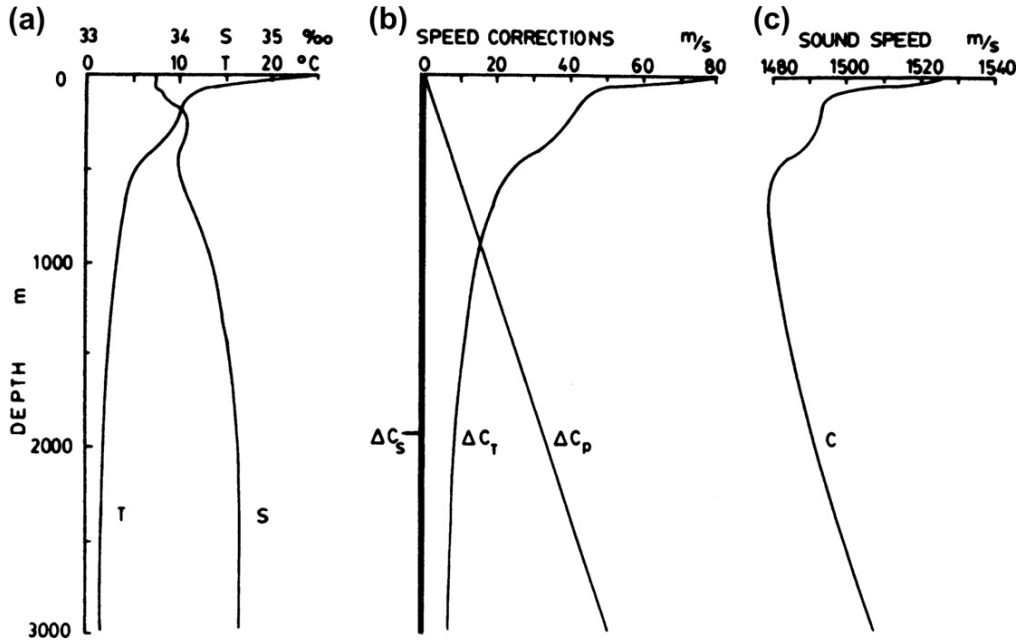

FIGURE 3.7 For station Papa in the Pacific Ocean at 39°N, 146°W, August, 1959: (a) temperature (°C) and salinity (psu) profiles, (b) corrections to sound speed due to salinity, temperature, and pressure, (c) resultant in situ sound-speed profile showing sound-speed minimum (SOFAR channel).

moderate angles above the horizontal are refracted downward, across the depth of the sound-speed minimum, and then refracted upward; they continue to oscillate about the sound-speed minimum depth. (Rays that travel steeply up or down from the source will not be channeled but may travel to the surface or bottom and be reflected there.) Low frequency sound waves (hundreds of hertz) can travel considerable distances (thousands of kilometers) along the SOFAR channel. This permits detection of submarines at long ranges and has been used for locating lifeboats at sea. Using the SOFAR channel to track drifting subsurface floats to determine deep currents is described in Chapter S6, Section S6.5.2 of the supplemental materials located on the textbook Web site.

The deep SOFAR channel of Figure 3.8b is characteristic of middle and low latitudes, where the temperature decreases substantially as depth increases. At high latitudes where the temperatures near the surface may be constant or even decrease toward the surface, the sound speed can have a surface minimum (Figure 3.8a). The much shallower sound channel, called a surface duct, may even be in the surface layer. In this case, downward directed sound rays from a shallow source are refracted upward while upward rays from the subsurface source are reflected downward from the surface and then refracted upward again. In this situation, detection of deep submarines from a surface ship using sonar equipment mounted in the hull may not be possible and deep-towed sonar equipment may be needed. In shallow water (e.g., bottom depth <200 m), reflection can occur both from the surface and from the bottom.

A pulse transmitted from a source near the SOFAR channel axis does not appear to

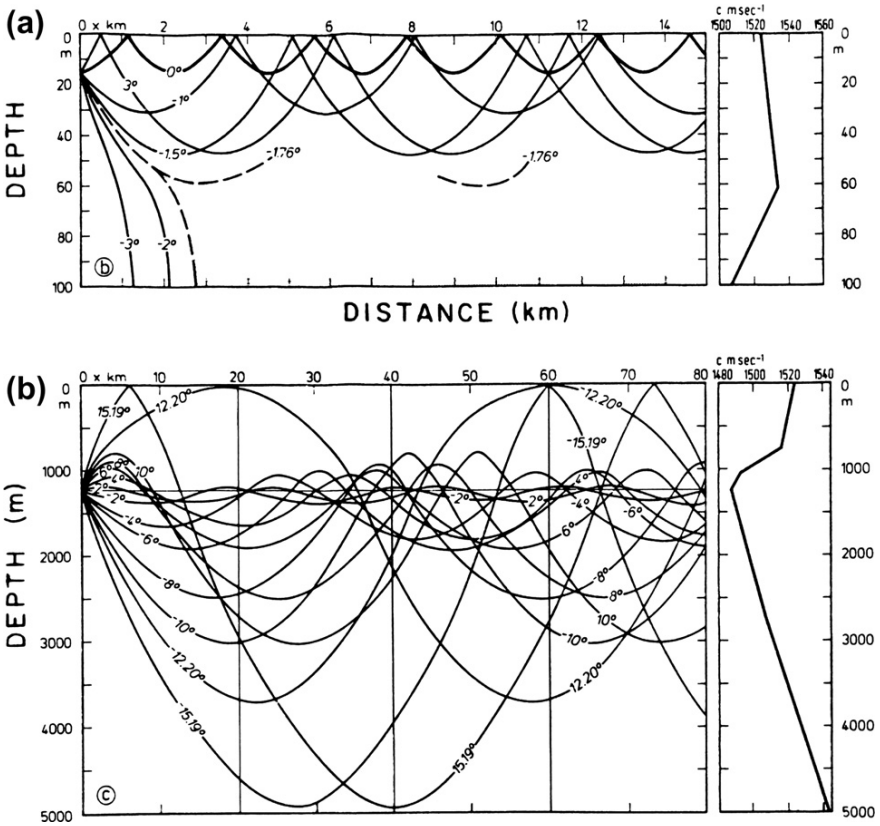

FIGURE 3.8 Sound ray diagrams: (a) from a shallow source for a sound-speed profile initially increasing with depth in upper mixed layer to a shallow minimum and then decreasing, and (b) from a sound source near the speed minimum in the sound channel for a typical open ocean sound-speed profile.

distant receivers as a sharp pulse but as a drawn-out signal rising slowly to a peak followed by a sharp cutoff. The peak before the cutoff is the arrival of the sound energy along the sound channel axis (direct signal), while the earlier arrivals are from sound that traveled along the refracted ray routes. It might appear in Figure 3.8b that the refracted rays have to travel a greater distance than the direct ray and would thus be delayed, but this is an illusion. Figure 3.8b is drawn with gross vertical exaggeration to enable the rays to be shown clearly, but the differences in distances traveled by refracted rays and the direct rays are very small; the greater speed in the refracted ray paths compensates for the greater distance they travel, so the direct ray arrives last.

Sound is used widely to locate and observe solid objects in the water. Echo sounders are used to measure bottom depths to the ocean's maximum depth of more than 11,000 m. SONAR (**SO**und **N**avigation **A**nd **R**anging) can determine the direction and distance to a submarine at ranges of hundreds of meters and to schools of fish at somewhat lesser ranges. Sidescan sonars determine the structure of the ocean bottom and can be used to locate shipwrecks. Acoustically tracked Swallow floats (see Chapter S6, Section S6.5.2 of the supplemental

material on the textbook Web site) provided some of the first direct observations of deep currents. Current speeds (or the speed of a ship relative to the water) are often measured using the reflection of sound waves from small particles moving with the water, applying the principle of Doppler shift. Because temperature and density affect the sound velocity, sound can be used to infer ocean water characteristics and their variations. Sound is used to measure surface processes such as precipitation, a measurement that is otherwise nearly impossible to determine.

In echo sounding, short pulses of sound energy are directed vertically downward where they reflect off of the bottom and return to the ship. (Echo sounders are also used to detect shoals of fish, whose air bladders are good reflectors of sound energy. Modern "fish finders" are simply low-cost echo sounders designed to respond to the fish beneath the vessel.) The acoustic travel time, t, yields the depth $D = C_o t/2$, where C_o is the mean sound speed between the surface and the bottom. Transducers in ordinary echo sounders are not much larger than the wavelength of the sound, so the angular width of the sound beam is large. Wide beams cannot distinguish the details of bottom topography. For special sounding applications, much larger sound sources that form a narrower beam are used. It is also possible to improve the resolution by using higher frequencies (up to 100 kHz or even 200 kHz), but the absorption of sound energy by seawater increases roughly as the square of the frequency, so higher frequency echo sounders cannot penetrate as deeply.

Inhomogeneities distort an initial sharp sound pulse so that the signal received at a hydrophone is likely to have an irregular tail of later arrival sounds. This is referred to as *reverberation*. One source of reverberation is the "deep scattering layer," which is biological in nature. This layer is characterized by diel (day/night) vertical migrations of several hundreds of meters; the organisms migrate toward the sea surface at dusk to feed and back down at dawn. This layer was first identified because of the scattering produced by the plankton and (gas-filled) fish bladders.

Sound is used to determine the speed of ocean currents and of ships, using a technique called acoustic Doppler profiling (see Chapter S6, Section S6.5.5.1 of the supplemental material located on the textbook Web site). Sound is transmitted from a source and reflects off the particles (mainly plankton) in the water and returns back to a receiver. If the source is moving relative to the particles, then the received sound wave has a different frequency from the transmitted wave, a phenomenon called Doppler shifting. Doppler shift is familiar to anyone who has listened to the sound of a siren when an emergency vehicle first approaches (Doppler shifting the sound to a higher frequency and, therefore, a higher pitch) and then retreats away (Doppler shifting the sound to a lower frequency and lower pitch). Acoustic Doppler speed logs are common on ships and give a relatively accurate measure of the speed of the ship through the water. If the ship's speed is tracked very precisely using, for instance, GPS navigation, then the ship speed can be subtracted from the speed of the ship relative to the water to yield the speed of the water relative to the GPS navigation, providing a measure of current speeds. Acoustic Doppler current profilers are also moored in the ocean to provide long-term records of current speeds.

Sound can be used to map the ocean's temperature structure and its changes, through a technique called acoustic tomography (see Chapter S6, Section S6.6.1 of the supplemental material located on the textbook Web site). Since sound speed depends on temperature, temperature changes along a ray path result in travel time changes. With extremely accurate clocks, these changes can be detected. If multiple ray paths crisscross a region, the travel time changes can be combined using sophisticated data analysis techniques to map temperature changes in

the region. This technique has been especially useful in studying the three-dimensional structure of deep convection in regions and seasons that are virtually impossible to study from research ships. Similar techniques have been applied to very long distance monitoring of basin-average ocean temperature, which is possible because of the lack of attenuation of sound waves over extremely long distances (Munk & Wunsch, 1982). However, large-scale monitoring of ocean temperature changes using sound has been eclipsed by the global temperature–salinity profiling float array, Argo, which provides local as well as basin-average information.

Much more information about ocean acoustics can be found in textbooks such as Urick (1983).

3.8. LIGHT AND THE SEA

This is a very brief introduction to a complex subject. Full treatments are available in various sources; some suggestions are Mobley (1995) and Robinson (2004).

Sunlight with a range of wavelengths enters the sea after passing through the atmosphere. Within the upper layer of the ocean, up to 100 m depth or more, the visible light interacts with the water molecules and the substances that are dissolved or suspended in the water. The light provides energy for photosynthesis and also heats the upper layer. Processes of backscattering, absorption, and re-emission result in the visible light (ocean color) that emerges back from the ocean surface into the atmosphere. This emerging radiation is then measured with instruments above the sea surface, including satellites. For satellite observations, the atmosphere again affects the signal from the sea. Observations of ocean color by satellites can then be related to the processes within the ocean that affect the emerging light, including an abundance of phytoplankton, particulate organic carbon, suspended sediment, and so forth.

Absorption (attenuation) of the sun's energy in the upper layer depends on the materials within the water; therefore these materials affect how heating is distributed in the surface layer and affects mixed layer processes. General circulation models that are run with observed forcing sometimes use information about light attenuation, affecting mixed layer formation and, consequently, sea surface temperature in the model.

Section 3.8.1 describes the optical properties of seawater and Section 3.8.2 describes the quantity that is observed as ocean color. Examples of observations are shown in Chapter 4.

3.8.1. Optical Properties

The sun irradiates the earth with a peak in the visible spectrum (wavelengths from about 400 to 700 nm, from violet to red, where 1 nm = 10^{-9} m). Sunlight behaves differently in water and air. The ocean absorbs light in much shorter distances than the atmosphere. When this shortwave energy penetrates the sea, some of it is scattered, but much is absorbed, almost all within the top 100 m. The energy is attenuated approximately exponentially. This is the photic (euphotic) zone, where photosynthesis occurs. This penetration of solar energy into the ocean's upper layer is also important in the ocean's heat budget (Chapter 5).

A schematic overview of the ocean's optical processes is shown in Figure 3.9, after Mobley (1995), who provides much greater detail and precise expressions for each of the quantities in the diagram. Each of the quantities can be observed, with greater or lesser difficulty. At the top of the diagram, the external environmental quantities that determine the amount of radiation entering the ocean are the sun's radiance distribution, which depends on its position and on sky conditions; the sea state, since this determines how much radiation is reflected without entering the sea; and the ocean bottom, if it is shallow enough to intercept the

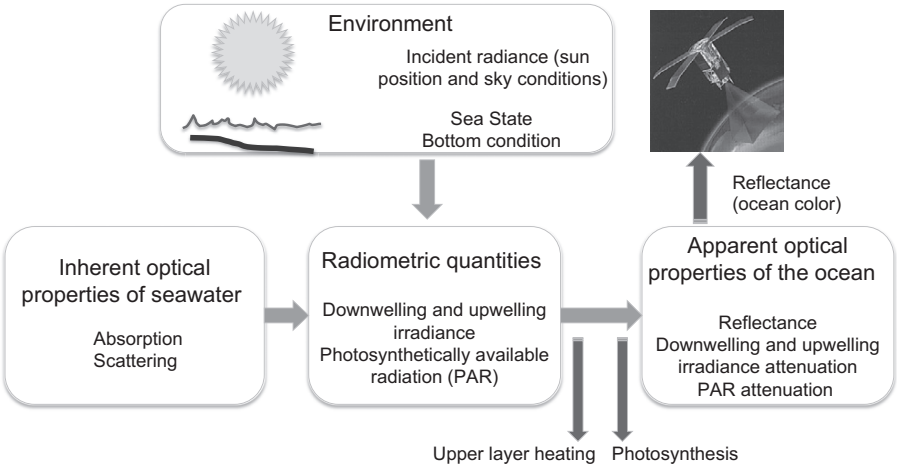

FIGURE 3.9 Schematic of optical processes in seawater. Adapted and simplified from Mobley (1995), with added indicators of seawater heating and photosynthesis, as well as satellite observation of ocean color.

light. The *inherent optical properties* of the seawater determine how it absorbs and scatters radiation, as a function of wavelength; this depends on the matter that is dissolved, suspended, or active (in the case of phytoplankton).

The environmental conditions and inherent optical properties work together through a radiative transfer equation to set the radiometric quantities of the medium. Here it is useful to provide some definitions of the radiometric quantities listed in the middle box of Figure 3.9. First, we note that light from a source, which could be at any point in a medium in which light is diffused or scattered, illuminates a complete sphere around the source. Therefore the solid angle, measured in "steradians" (sr), is a useful measure, similar to area. Next, the flux of energy from the light is measured in Watts (J/sec). The *radiance* is the flux of energy per unit area and per unit steradian; it is measured in units of $W/(sr\ m^2)$. If the radiance is measured as a function of wavelength of the light (i.e., spectral radiance), then its units are $W/(sr\ m^2\ nm)$ if wavelength is measured in nanometers.

The *irradiance* is the total amount of radiance that reaches a given point (i.e., where your optical measurement is made), so it is the sum of radiance coming in from all directions to the observation point; therefore it is the integral of radiance over all solid angles, and has units of W/m^2 for total irradiance, or $W/(m^2\ nm)$ for spectral irradiance (which is a function of wavelength). Next, *upwelling* irradiance is defined as the irradiance from all solid angles below the observation point; downwelling irradiance would come from all angles above that point.

Reflectance is the ratio of upwelling irradiance to downwelling irradiance, defined at a point; reflectance defined this way has no units. It is not the same as actual reflected light from the sea surface. Rather, reflectance is the light emerging from the ocean. For remote sensing, in which the radiation from the ocean's surface is being measured from a specified location, rather than from all directions, reflectance can be defined alternatively as the ratio of upwelling radiance to downwelling irradiance; in this case, reflectance has units of (sr^{-1}).

Finally, the amount of radiation available for photosynthesis (photosynthetically available radiation; PAR) is measured in photons $s^{-1}\ m^{-2}$.

Returning to Figure 3.9, the rightmost bottom box lists the *apparent optical properties* of the seawater. These include the rate at which light is attenuated within the water column, and how much light returns back out through the

sea surface (indicated as reflectance). The irradiance and PAR are attenuated with increasing depth as the radiation is absorbed, scattered, and used for photosynthesis by phytoplankton. Attenuation is often approximately exponential. If attenuation were exactly exponential, of the form $I(z) = I_o\ e^{-Kz}$, where I_o is the radiation intensity at the sea surface, I the intensity at a depth z meters below the surface, and K the vertical attenuation coefficient of the water, then the apparent optical properties would be expressed in terms of the e-folding depth, K. The actual attenuation is not exponential, so the attenuation coefficient, K, is proportional to the depth derivative of the radiation intensity (and would be equal to the e-folding depth if the dependence were exponential).

The effects of depth and constant attenuation coefficient on light intensity are illustrated in Table 3.3, from Jerlov (1976). The coefficient K depends mainly on factors affecting absorption of light in the water and to a lesser extent on scattering. The last two columns of Table 3.3 indicate the range of penetrations found in actual seawater.

The smallest attenuation coefficient in Table 3.3 ($K = 0.02\ m^{-1}$) represents the clearest ocean water and deepest penetration of light energy. Energy penetrates coastal waters less readily because of the extra attenuation due to suspended particulate matter and dissolved materials. The largest attenuation coefficient listed in the table, $K = 2\ m^{-1}$, represents very turbid water with many suspended particles.

In seawater, the attenuation coefficient K also varies considerably with wavelength. Figure 3.10b shows the relative amounts of energy penetrating clear ocean water to 1, 10, and 50 m as a function of wavelength (solid curves). Light with blue wavelengths penetrates deepest; penetration by yellow and red is much less. That is, blue light, with wavelength of about 450 nm, has the least attenuation in clear ocean water. At shorter and longer wavelengths (in the ultraviolet and red), the attenuation is much greater. The increased attenuation in the ultraviolet is not important to the ocean's heat budget, because the amount of energy reaching sea level at such short wavelengths is small. Much more solar energy is contained in and beyond the red end of the spectrum. Virtually all of the energy at wavelengths shorter than the visible is absorbed in the top meter of water, while the energy at long wavelengths (1500 nm or greater) is absorbed in the top few centimeters.

All wavelengths are attenuated more in turbid water than in clear water. In clear ocean

TABLE 3.3 Amount of Light Penetrating to Specified Depths in Seawater as a Percentage of that Entering Through the Surface

	Vertical Attenuation Coefficient K (m^{-1})			**Clearest Ocean Water**	**Turbid Coastal Water**
Depth (m)	K = 0.02	K = 0.2	K = 2		
0	100%	100%	100%	100%	100%
1	98	82	14	45	18
2	96	67	2	39	8
10	82	14	0	22	0
50	37	0	0	5	0
100	14	0	0	0.5	0

Jerlov, 1976.

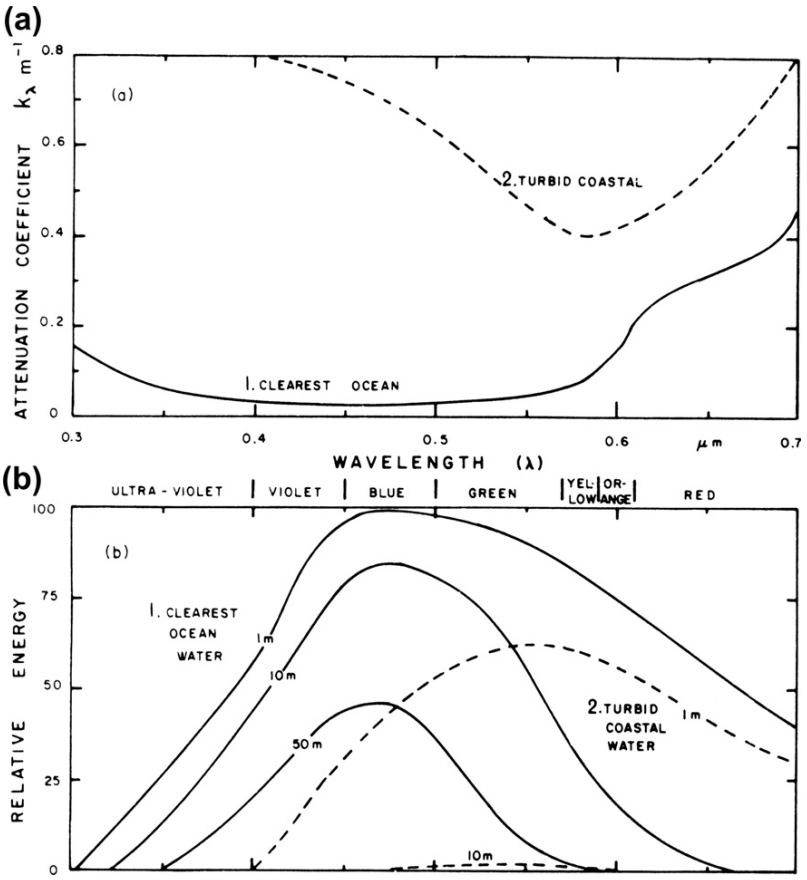

FIGURE 3.10 (a) Attenuation coefficient k_λ, as a function of wavelength λ (μm) for clearest ocean water (solid line) and turbid coastal water (dashed line). (b) Relative energy reaching 1, 10, and 50 m depth for clearest ocean water and reaching 1 and 10 m for turbid coastal waters.

water, there is enough light at 50 to 100 m to permit a diver to work, but in turbid coastal waters almost all of the energy may have been absorbed by a depth of 10 m. K is larger for turbid water than clear (Figure 3.10a), and the least attenuation is in the yellow part of the spectrum. In turbid water, less energy penetrates to 1 m and 10 m, and the maximum penetration is shifted to the yellow (Figure 3.10b). (The energy reaching 50 m in this turbid water is too small to show on the scale of this graph.)

In clear ocean water, the superior penetration of blue and green light is evident both visually when diving and also in color photographs taken underwater by natural light. Red or yellow objects appear darker in color or even black as they are viewed at increasing depths because the light at the red end of the spectrum has been absorbed in the upper layers and little is left to be reflected by the objects. Blue or green objects retain their colors to greater depths.

The presence of plankton in seawater also changes the penetration depth of solar radiation, and hence the depth at which the sun's heat is absorbed. This changes the way the surface mixed layer develops, which can in turn impact the plankton, leading to a feedback. There are significant and permanent geographical variations in this vertical distribution of absorption, since some regions of the world

ocean have much higher biological productivity than others.

3.8.2. Ocean Color

To the eye, the color of the sea ranges from deep blue to green to greenish yellow (Jerlov, 1976). Broadly speaking, deep or indigo blue color is characteristic of tropical and equatorial seas, particularly where there is little biological production. At higher latitudes, the color changes through green-blue to green in polar regions. Coastal waters are generally greenish.

Two factors contribute to the blue color of open ocean waters at low latitudes. Because water molecules scatter the short-wave (blue) light much more than the long-wave (red) light, the color seen is selectively blue. In addition, because the red and yellow components of sunlight are rapidly absorbed in the upper few meters, the only light remaining to be scattered by the bulk of the water is blue. Looking at the sea from above, sky light reflected from the surface is added to the blue light scattered from the body of the water. If the sky is blue, the sea will still appear deep blue, but if there are clouds, the white light reflected from the sea surface dilutes the blue scattered light from the water and the sea appears less intensely blue.

If there are phytoplankton in the water, their chlorophyll absorbs blue light and also red light, which shifts the water color to green. (This is also why plants are green.) The organic products from plants may also add yellow dyes to the water; these will absorb blue and shift the apparent color toward the green. These shifts in color generally occur in the more productive high-latitude and coastal waters. In some coastal regions, rivers carry dissolved organic substances that emphasize the yellowish green color. The red color that occurs sporadically in some coastal areas, the so-called red tide, is caused by blooms of reddish brown phytoplankton. Mud, silt, and other finely divided inorganic materials carried into the ocean by rivers can impart their own color to the water. In some fjords, the low-salinity surface layer may be milky white from the finely divided "rock flour" produced by abrasion in the glaciers and carried down by the melt water. The sediment can be kept in suspension by turbulence in the upper layer for a time, but when it sinks into the saline water, it flocculates (forms lumps) and sinks more rapidly. When diving in such a region the diver may be able to see only a fraction of a meter in the upper layer but be able to see several meters in the saline water below.

The color of seawater and depth of penetration of light were traditionally judged using a white Secchi disk (see Chapter S6, Section S6.8 of the supplemental materials located on the textbook Web site) lowered from the ship. This method has been superseded by a suite of instruments that measure light penetration at different wavelengths, transparency of the water at various wavelengths, and fluorescence. Most important, color observations are now made continuously and globally by color sensors on satellites.

Ocean color is a well-defined quantity, related to reflectance (Figure 3.9 and definition in Section 3.8.1). Reflectance, or ocean color, can be measured directly above the ocean's surface. Observations of ocean color since the 1980s have been made from satellites, and must be corrected for changes as the light passes upward through the atmosphere. Ocean color observations are then converted, through complex algorithms, to physically useful quantities such as the amount of chlorophyll present, or the amount of particulate organic carbon, or the amount of "yellow substance" (gelbstoff) that is created by decaying vegetation. With global satellite coverage, these quantities can be observed nearly continuously and in all regions.

Robinson (2004) provided a complete treatment of the optical pathways involved in ocean

color remote sensing, starting with consideration of the total radiance observed by the satellite sensor. Many pathways contribute to the observed radiance. These can be grouped into an atmospheric path radiance (L_p), a "water-leaving radiance" from just below the sea surface (L_w), and a radiance due to all surface reflections (L_r) within the instantaneous field of view of the satellite sensor. The radiance L_s received at the satellite sensor is

$$L_s = L_p + TL_w + TL_r \qquad (3.15)$$

T is the transmittance, which gives the proportion of radiance that reaches the sensor without being scattered out of the field of view.

The water-leaving radiance provides the information about ocean color, so it is the desired observed quantity. It is closely related to the reflectance; the ratio of water-leaving radiance just above the sea surface to downwelling irradiance incident on the sea surface is the "remote sensing reflectance," or "normalized water-leaving radiance." The three net radiance terms depend on the wavelength and on the turbidity of the seawater. The largest contribution is from the atmospheric pathway L_p. The water-leaving and reflected radiances are much smaller. Because of the weak signal strength for the ocean pathways (water-leaving radiance), ocean color remote sensing requires very precise atmospheric correction of the visible light sensed by the satellite. Complex radiative transfer models are invoked to carry out this correction and often the accuracy of the chlorophyll estimates depends critically on this atmospheric correction. After correction, the resultant radiances are analyzed for various components related to biological activity, particularly chlorophyll.

The biggest effect of chlorophyll on the spectrum of reflectance (normalized water-leaving radiance) is to reduce the energy at the blue end of the spectrum compared with the spectrum for clear water. This is demonstrated in Figure 3.11 (H. Gordon, personal communication, 2009). Here the spectrum of radiance is shown with and without correction for the atmosphere. When the atmosphere is not removed, there is virtually no difference between the spectra for low and high chlorophyll waters. When the atmospheric signal is

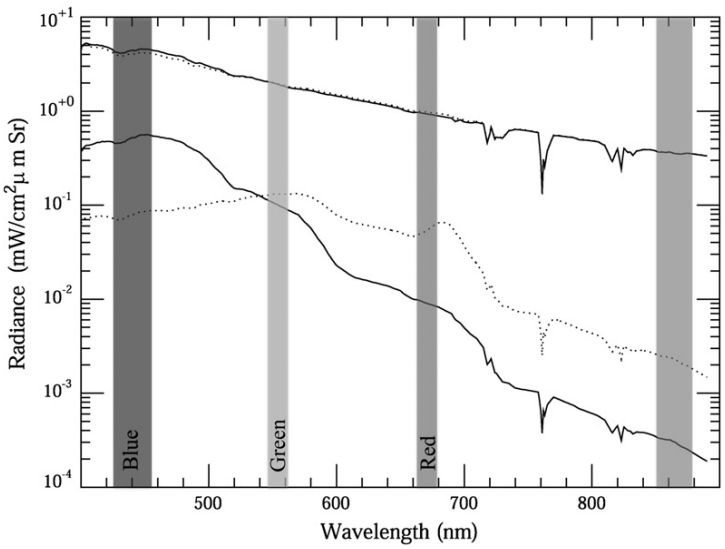

FIGURE 3.11 Example of observations of water-leaving radiance observed by the Multi-angle Imaging SpectroRadiometer (MISR), with bands observed by satellite color sensors indicated. Solid curves: low chlorophyll water (0.01 mg/m^3). Dotted curves: high chlorophyll water (10.0 mg/m^3). The two lower curves have the atmospheric signal removed. (H. Gordon, personal communication, 2009.)

removed, the desired difference emerges. The high chlorophyll spectrum is depressed at the blue end of the spectrum and elevated at the green and red.

Ocean color observations from satellites can also be used as a proxy for the attenuation properties of seawater, which can be used in mixed layer models that are set up to be run with observed atmospheric forcing. Absorption of solar radiation in the ocean heats the upper layer. The time and space distribution of absorption is directly related to the substances in the water column, and this affects ocean color. In practice, at present most mixed layer models in ocean general circulation models use a sum of two exponentially decaying functions that are proxies for attenuation of red light (quickly absorbed) and blue-green light (penetrating much deeper), with coefficients based on assumption of a particular Jerlov (1976) water type (Paulson & Simpson, 1977). However, explicit incorporation of biological effects on attenuation (incorporation of ocean color observations and of bio-optical models along with mixed layer models) is being tested widely and is a likely direction for the future, since the effects on modeled mixed layer temperature are clear (Wu, Tang, Sathyendranath, & Platt, 2007) and can in fact affect the temperature of the overlying atmosphere (Shell, Frouin, Nakamoto, & Somerville, 2003).

3.9. ICE IN THE SEA

Ice in the sea has two origins: the freezing of seawater and the ice broken off from glaciers. The majority of ice comes from the first of these sources and is referred to as *sea ice*; the glaciers supply "pinnacle" icebergs in the Northern Hemisphere and flat "tabular" icebergs in the Southern Hemisphere. Sea ice alters the heat and momentum transfers between the atmosphere and the ocean, is a thermal insulator, damps surface waves, changes the temperature and salinity structure in the upper layer by melting and freezing, and is a major hindrance to navigation. Ice cover is an important part of Earth's climate feedbacks because of its high reflectivity, that is, its high *albedo* (Section 5.4.3). The ice–albedo feedback, which affects climate, is described in Section 5.4.5, and is especially important in the Arctic (Section 12.8).

3.9.1. Freezing Process

When water loses sufficient heat (by radiation, conduction to the atmosphere, convection, or evaporation) it freezes to ice, in other words, it changes to the solid state. Initial freezing occurs at the surface and then the ice thickens by freezing at its lower surface as heat is conducted away from the underlying water through the ice to the air.

The initial freezing process is different for fresh and low-salinity water than for more saline water because the temperature at which water reaches its maximum density varies with salinity. Table 3.4 gives the values of the freezing point and temperature of maximum density for water of various salinities. (Note that the values are for freezing, etc., at atmospheric pressure. Increased pressure lowers the freezing point, which decreases by about 0.08 K per 100 m increase in depth in the sea.)

To contrast the freezing process for freshwater and seawater, first imagine a freshwater lake where the temperature initially decreases from about 10°C at the surface to about 5°C

TABLE 3.4 Temperatures of the Freezing Point (t_f) and of Maximum Density ($t_{\rho max}$) for Fresh and Salt Water

S	0	10	20	24.7	30	35 psu
t_f	0	−0.5	−1.08	−1.33	−1.63	−1.91°C
$t_{\rho max}$	+3.98	+1.83	−0.32	−1.33	—	−°C

Note that the values for freezing and so forth are at atmospheric pressure. Increased pressure lowers the freezing point, which decreases by about 0.08 K per 100 m increase in depth in the sea.

at about 30 m depth. As heat is lost through the surface, the density of the water increases and vertical convective mixing (overturn) occurs with the temperature of the surface water layer gradually decreasing. This continues until the upper mixed layer cools to 3.98°C and then further cooling of the surface water causes its density to decrease and it stays near the top. The result is a rapid loss of heat from a thin surface layer, which soon freezes. For seawater of salinity = 35 psu of the same initial temperature distribution, surface cooling first results in a density increase and vertical mixing by convention currents occurs through a gradually increasing depth, but it is not until the whole column reaches −1.91°C that freezing commences. As a much greater volume of water has to be cooled through a greater temperature range than in the freshwater case, it takes longer for freezing to start in salt water than in freshwater. A simple calculation for a column of freshwater of 100 cm depth and 1 cm^2 cross-section initially at 10°C shows that it takes a heat loss of l63 J to freeze the top 1 cm layer, whereas for a similar column of seawater of S = 35 psu it takes a loss of 305 J to freeze the top 1 cm because the whole column has to be cooled to −1.91°C rather than just the top 1 cm to 0°C for the freshwater.

Note that as seawater of salinity <24.7 psu has a higher temperature of maximum density than its freezing point, it will behave in a manner similar to freshwater, although with a lower freezing point. For seawater of salinity >24.7 psu, (in high latitudes) the salinity generally increases with depth, and the stability of the water column usually limits the depth of convection currents to 30−50 m. Therefore ice starts to form at the surface before the deep water reaches the freezing point.

Generally, sea ice forms first in shallow water near the coast, particularly where the salinity is reduced by river runoff and where currents are minimal. When fully formed, this sea ice connected to the shore is known as "fast ice." The first process is the formation of needle-like crystals of pure ice, which impart an "oily" appearance to the sea surface (grease or frazil ice). The crystals increase in number and form a slush, which then thickens and breaks up into pancakes of approximately one meter across. With continued cooling, these pancakes grow in thickness and lateral extent, eventually forming a continuous sheet of floe or sheet ice.

Once ice has formed at the sea surface, when the air is colder than the water below, freezing continues at the lower surface of the ice and the rate of increase of ice thickness depends on the rate of heat loss upward through the ice (and any snow cover). This loss is directly proportional to the temperature difference between top and bottom surfaces and inversely proportional to the thickness of the ice and snow cover.

With very cold air, a sheet of sea ice of up to 10 cm in thickness can form in 24 hours, the rate of growth then decreasing with increasing ice thickness. Snow on the top surface insulates it and reduces the heat loss markedly, depending on its degree of compaction. For instance, 5 cm of new powder snow may have insulation equivalent to 250−350 cm of ice, while 5 cm of settled snow can be equivalent to only 60−100 cm of ice, and 5 cm of hard-packed snow can be equivalent to only 20−30 cm of ice.

As an example of the annual cycle of the development of an ice sheet at a location in the Canadian Arctic, ice was observed to start to form in September, was about 0.5 m thick in October, 1 m in December, 1.5 m in February, and reached its maximum thickness of 2 m in May—after which it started to melt.

3.9.2. Brine Rejection

In the initial stage of ice-crystal formation, salt is rejected and increases the density of the neighboring seawater, some of which then tends to sink and some of which is trapped among the ice crystals forming pockets called "brine cells."

The faster the freezing, the more brine is trapped. Sea ice in bulk is therefore not pure water-ice but has a salinity of as much as 15 psu for new ice (and less for old ice because gravity causes the brine cells to migrate downward in time). With continued freezing, more ice freezes out within the brine cells leaving the brine more saline, in a process called *brine rejection*. Some of the salts may even crystallize out.

Because of brine rejection, the salinity of first-year ice is generally 4–10 psu, for second-year ice (ice that has remained frozen beyond the first year) salinity decreases to 1–3 psu, and for multiyear ice salinity may be less than 1 psu. If sea ice is lifted above sea level, as happens when ice becomes thicker or rafting occurs, the brine gradually trickles down through it and eventually leaves almost salt-free, clear old ice. Such ice may be melted and used for drinking whereas melted new ice is not potable. Sea ice, therefore, is considered a material of variable composition and properties that depends very much on its history. (For more detail see Doronin & Kheisin, 1975.)

As a result of brine rejection, the salinity of the unfrozen waters beneath the forming sea ice increases. When this occurs in shallow regions, such as over continental shelves, the increase in salinity can be marked and can result in formation of very dense waters. This is the dominant mechanism for formation of the deep and bottom waters in the Antarctic (Chapter 13), and for formation of the densest part of the North Pacific Intermediate Water in the Pacific (Chapter 10). Brine rejection is a central process for modification of water masses in the Arctic as well (Chapter 12).

3.9.3. Density and Thermodynamics of Sea Ice

The density of pure water at 0°C is 999.9 kg/m^3 and that of pure ice is 916.8 kg/m^3. However the density of sea ice may be greater than this last figure (if brine is trapped among the ice crystals) or less (if the brine has escaped and gas bubbles are present.) Values from 924 to 857 kg/m^3 were recorded on the Norwegian Maud Expedition (Malmgren, 1927).

The amount of heat required to melt sea ice varies considerably with its salinity. For S = 0 psu (freshwater ice) it requires 19.3 kJ/kg from −2°C and 21.4 kJ/kg from −20°C, while for sea ice of S = 15 psu, it requires only 11.2 kJ/kg from −2°C but 20.0 kJ/kg from −20°C. The small difference of heat (2.1 kJ/kg) needed to raise the temperature of freshwater ice from −20°C to −2°C is because no melting takes place; that is, it is a true measure of the specific heat of pure ice. However, for sea ice of S = 15 psu, more heat (8.8 kJ/kg) is required to raise its temperature through the same range, because some ice near brine cells melts and thus requires latent heat of melting as well as heat to raise its temperature. Note also that less heat is needed to melt new ice (S = 15 psu) than old ice, which has a lower salinity.

3.9.4. Mechanical Properties of Sea Ice

Because of the spongy nature of first-year sea ice (crystals + brine cells) it has much less strength than freshwater ice. Also, as fast freezing results in more brine cells, the strength of ice formed this way is less than when freezing occurs slowly; in other words, sea ice formed in very cold weather is initially weaker than ice formed in less cold weather. As the temperature of ice decreases, its hardness and strength increase, and ice becomes stronger with age as the brine cells migrate downward. When ice forms in calm water, the crystals tend to line up in a pattern and such ice tends to fracture along cleavage planes more easily than ice formed in rough water where the crystals are more randomly arranged and cleavage planes are not formed.

The mechanical behavior of sea ice is complex when temperature changes. As the ice temperature decreases below its freezing point, the ice expands initially, reaches a maximum

expansion, and then contracts. For instance, an ice floe of S = 4 psu will expand by 1 m per 1 km length between −2 and −3°C, reaches its maximum expansion at −10°C, and thereafter contracts slightly. Ice of S = 10 psu expands 4 m per 1 km length from −2 to −3°C, and reaches its maximum expansion at −18°C. The expansion on cooling can cause an ice sheet to buckle and "pressure ridges" to form, while contraction on further cooling after maximum expansion results in cracks, sometimes wide, in the ice sheet.

Pressure ridges can also develop as a result of wind stress on the surface driving ice sheets together. The ridges on top are accompanied by a thickening of the lower surface of the ice by four to five times the height of the surface ridges. Sea ice generally floats with about five-sixths of its thickness below the surface and one-sixth above, so relatively small surface ridges can be accompanied by deep ridges underneath — depths of 25 to 50 m below the sea surface have been recorded. Thickening of an ice sheet may also result from rafting when wind or tide forces one ice sheet on top of another or when two sheets, in compression, crumble and pile up ice at their contact. Old ridges, including piled up snow, are referred to as *hummocks*. As they are less saline than newer pressure ridges, they are stronger and more of an impediment to surface travels than the younger ridges.

3.9.5. Types of Sea Ice and its Motion

Sea ice can be categorized as fast ice (attached to the shore), pack ice (seasonal to multiyear ice with few gaps), and cap ice (thick, mostly multi-year ice), as described in Section 12.7.1. Several forces determine the motion of sea ice if it is not landfast:

(a) Wind stress at the top surface (the magnitude depending on the wind speed and the roughness of the ice surface as ridges increase the wind stress). Typical ice speeds are 1 to 2% of the wind speed.

(b) Frictional drag on the bottom of an ice sheet moving over still water tends to slow it down, while water currents (ocean and tidal) exert a force on the bottom of the ice in the direction of the current. Because current speeds generally decrease with increase in depth, the net force on deep ice and icebergs will be less than on thin ice, and pack ice will move past icebergs when there is significant wind stress.

(c) In the cases of (a) and (b), the effect of the Coriolis force (Section 7.2.3) is to divert the ice motion by 15−20 degrees to the right of the wind or current stress in the Northern Hemisphere (to the left in the Southern Hemisphere). (It was the observation of the relation between wind direction and ice movement by Nansen, and communicated by him to Ekman, that caused the latter to develop his well-known theory of wind-driven currents.) It is convenient to note that as surface friction causes the surface wind to blow at about 15 degrees to the left of the surface isobars, the direction of the latter is approximately that in which the ice is likely to drift (Northern Hemisphere).

(d) If the ice sheet is not continuous, collisions between individual floes may occur with a transfer of momentum (i.e., decrease of speed of the faster floe and increase of speed of the slower). Energy may go into ice deformation and building up ridges at impact. This is referred to as internal ice resistance and increases with ice concentration, that is, the proportion of area covered by ice. The effect of upper surface roughness (R on a scale of 1 to 9) and ice concentration (C on a scale of 1 to 9) on the speed of the ice V (expressed as a percentage of the wind speed) is given by: $V = R(1 - 0.08°C)$ (taken to only one decimal place), so that the speed of the ice increases with

roughness but decreases with increased ice concentration. Note that for very close pack ice, stresses of wind or current are integrated over quite large areas and the local motion may not relate well to the local wind.

3.9.6. Polynyas and Leads

Regions of nearly open water within the ice pack are often found where one might expect to find ice. These open water areas are critical for air–sea heat exchange, since ice is a relatively good insulator. Small breaks between ice floes are called *leads*; these are created by motion of the ice pack and have random locations. Larger recurrent open water areas are called *polynyas*. There are two types of polynyas, depending on the mechanism maintaining the open water (Figure 3.12; see also Barber & Massom, 2007):

1. *Latent heat polynyas* are forced open by winds, often along coasts or ice shelf edges. New ice soon forms; latent heat from the forming sea ice is discharged to the atmosphere at a rate of as much as 200–500 W/m^2.
2. *Sensible heat polynyas* result from relatively warm water upwelling to the surface and melting the ice there. Another term often encountered is *flaw polynya*, which means that the polynya occurs at the boundary between fast ice and pack ice. Because most polynyas include a mixture of these forcings, nomenclature is tending toward being more specific about the forcing (mechanical–wind; convective–melting: Williams, Carmack, & Ingram, 2007).

Wind-forced polynyas are usually near coastlines or the edges of ice shelves or fast ice, where winds can be very strong, often forced by strong land–sea temperature differences (katabatic winds). The open water is often continually freezing in these polynyas since they are kept open through mechanical forcing. These wind-forced polynyas act as ice factories, producing larger amounts of new ice than regions where the ice is thicker and air–sea fluxes are minimized by the ice cover. If these polynyas occur over shallow continental shelves, the brine rejected in the ongoing sea ice formation process, together with temperatures at the

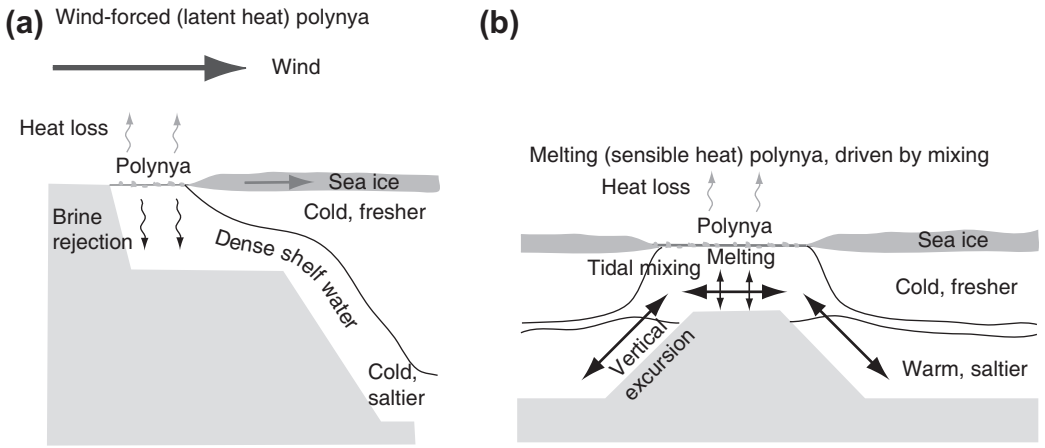

FIGURE 3.12 Schematics of polynya formation: (a) latent heat polynya kept open by winds and (b) sensible heat polynya kept open by tidal mixing with warmer subsurface waters (after Hannah et al., 2009).

freezing point, can produce especially dense shelf waters. This is one of the major mechanisms for creating very dense waters in the global ocean (Section 7.11), particularly around the coastlines of Antarctica (Chapter 13) and the Arctic (Chapter 12), as well as the densest (intermediate) water formed in the North Pacific in the Okhotsk Sea (Chapter 10).

Polynyas that are maintained by melting within the ice pack result from mixing of the cold, fresh surface layer with underlying warmer, saltier water. These polynyas might also produce sea ice along their periphery since the air–sea fluxes will be larger than through the ice cover, but the upward heat flux from the underlying warmer water means that they produce new ice much less efficiently than wind-forced polynyas. The vertical mixing can result from convection within the polynya, which can occur in deep water formation sites such as the Odden-Nordbukta in the Greenland Sea (Section 12.2.3). In shallow regions, the mixing process can be greatly enhanced by tides moving the waters over undersea banks (Figure 3.12b). A number of the well-known polynyas in the Canadian Archipelago in the Arctic Ocean are tidally maintained (Figure 12.23 from Hannah, Dupont, & Dunphy, 2009), as is a recurrent polynya over Kashevarov Bank in the Okhotsk Sea (Figure 10.29).

3.9.7. Ice Break-up

Ice *break-up* is caused by wave action, tidal currents, and melting. Melting of ice occurs when it gains enough heat by absorption of solar radiation and by conduction from the air and from nearby seawater to raise its temperature above the melting point. The absorption of radiation depends on the albedo of the surface (proportion of radiation reflected), which varies considerably; for example, the albedo for seawater is from 0.05 to 0.10 (it is a very good absorber of radiation), for snow-free sea ice it is from 0.3 to 0.4, while for fresh snow it is 0.8 to 0.9. Dark materials, like dirt and dust, have a low albedo of 0.1 to 0.25 and absorb radiation well. Such material on ice can form a center for the absorption of radiation and consequent melting of ice around it, so puddles can form. These can absorb heat because of the low albedo of water and may even melt right through an ice sheet. When any open water forms, it absorbs heat and causes rapid melting of ice floating in it.